

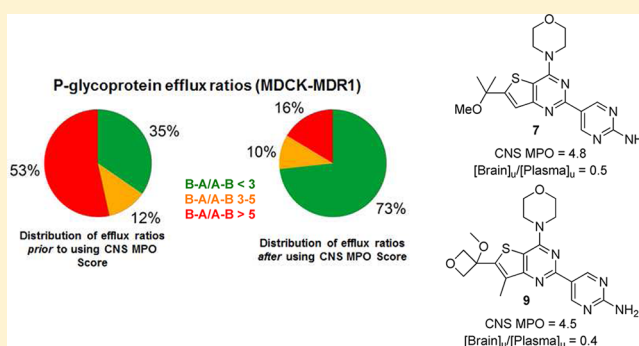
## The Design and Identification of Brain Penetrant Inhibitors of Phosphoinositide 3-Kinase $\alpha$

Timothy P. Heffron,\* Laurent Salphati, Bruno Aliche, Jonathan Cheong, Jennafer Dotson, Kyle Edgar, Richard Goldsmith, Stephen E. Gould, Leslie B. Lee, John D. Lesnick, Cristina Lewis, Chudi Ndubaku, Jim Nonomiya, Alan G. Olivero, Jodie Pang, Emile G. Plise, Steve Sideris, Sean Trapp, Jeffrey Wallin, Lan Wang, and Xiaolin Zhang

Genentech, Inc., 1 DNA Way, South San Francisco, California 94080, United States

### **S** Supporting Information

**ABSTRACT:** Inhibition of phosphoinositide 3-kinase (PI3K) signaling through PI3K $\alpha$  has received significant attention for its potential in cancer therapy. While the PI3K pathway is a well-established and widely pursued target for the treatment of many cancer types due to the high frequency of abnormal PI3K signaling, glioblastoma multiforme (GBM) is particularly relevant because the pathway is implicated in more than 80% of GBM cases. Herein, we report the identification of PI3K inhibitors designed to cross the blood–brain barrier (BBB) to engage their target where GBM tumors reside. We leveraged our historical experience with PI3K inhibitors to identify correlations between physicochemical properties and transporter efflux as well as metabolic stability to focus the selection of molecules for further study.



### ■ INTRODUCTION

Aberrant signaling through the phosphatidylinositol 3-kinase (PI3K) pathway is a prevalent phenomenon in numerous cancer types and has received significant attention as a drug target.<sup>1</sup> Dysregulated PI3K signaling may result from PI3K $\alpha$  amplification, PI3K $\alpha$  mutation, or loss of function of phosphatase and tensin homologue (PTEN), a negative regulator of PI3K. While the PI3K pathway is an attractive target for the treatment of many cancer types due to the high frequency of abnormal PI3K signaling, glioblastoma multiforme (GBM) is particularly relevant because the pathway is implicated in more than 80% of GBM cases.<sup>2,3</sup>

We were interested in addressing the unmet medical need for GBM patients through identification of PI3K inhibitors capable of penetrating the blood–brain barrier (BBB). Our previous programs in identifying inhibitors of PI3K led to the discoveries of the pan-PI3K inhibitor GDC-0941 (**1**)<sup>4</sup> and dual PI3K/mTOR inhibitors GNE-493 (**2**)<sup>5</sup> and GDC-0980 (**3**).<sup>6</sup> We began our study toward brain penetrant inhibitors of PI3K with **1–3** as well characterized and attractive molecules designed for systemic circulation. However, **1–3** were determined to very poorly penetrate the BBB ([brain]<sub>u</sub>/[plasma]<sub>u</sub>, Table 1), a phenomenon attributed to efflux by the two most prevalent transporters expressed at the BBB, P-glycoprotein (P-gp), and breast cancer resistance protein (Bcrp1) (efflux measured as the B–A/A–B ratio in permeability assays using multidrug resistance gene (MDR1) or Bcrp1 transfected Madin–Darby

canine kidney (MDCK) cells respectively).<sup>7</sup> We were particularly convinced that the action of both of these transporters was important to consider for this series of molecules, as studies of **1** in P-gp or Bcrp1 knockout mice had resulted in modest improvements of brain exposure but in mice lacking both transporters **1** achieved a high brain-to-plasma concentration ratio.<sup>8</sup>

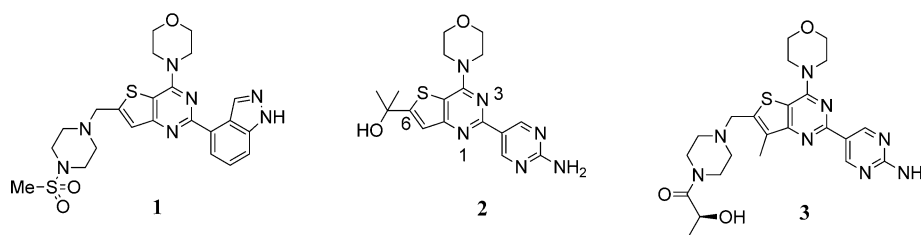
The poor BBB penetration and transporter mediated efflux experienced by compounds **1–3**, while disappointing, was not unexpected given how different their physicochemical properties are from marketed drugs that target the central nervous system (CNS; Table 2).<sup>9</sup> Compound **1** has a much higher topological polar surface area (TPSA) and molecular weight (MW) more than 200 units higher than the median value of 119 marketed CNS drugs. Compound **3** similarly contrasts with marketed CNS drugs but also has an additional two hydrogen bond donors (HBD). Compound **2**, while closer to the median MW of marketed CNS drugs, has three HBD and a much higher TPSA.

### ■ RESULTS AND DISCUSSION

Using compounds **1–3** as the “lead” matter for this program but wanting to move into physicochemical property space more consistent with CNS drugs, we decided to evaluate how much

Received: June 20, 2012

Published: September 4, 2012

**Table 1.** In Vitro Permeability Efflux Ratios from MDR1 and Bcrp1 Transfected MDCK Cell Line Assays and in Vivo Brain-to-Plasma Ratios for Compounds 1–3<sup>a</sup>

compd	B–A/A–B (MDR1)	B–A/A–B (Bcrp1)	[Brain]/[Plasma]	[Brain] <sub>u</sub> /[Plasma] <sub>u</sub> <sup>b</sup>
1	27	80	<0.05 <sup>c</sup>	<0.05
2	5	37	0.20 <sup>d</sup>	0.04
3	19	7	<0.10 <sup>e</sup>	<0.05

<sup>a</sup>All [Brain]/[Plasma] ratios determined after oral dose of female nu/nu mice with the indicated compound as an MCT suspension. <sup>b</sup>[Brain]<sub>u</sub> and [Plasma]<sub>u</sub> refer to the unbound concentration measured in the brain and plasma, respectively. <sup>c</sup>Determined after administration of 10 mg/kg and [Brain]/[Plasma] determined at 0.5 h. <sup>d</sup>Determined after administration of 15 mg/kg and [Brain]/[Plasma] determined at 0.5 h. <sup>e</sup>Determined after administration of 20 mg/kg at 1 h.

**Table 2.** Comparison of Calculated Physicochemical Properties of Compounds 1–3 with Marketed CNS Targeting Drugs<sup>a</sup>

compd	MW	HBD	TPSA	cLogP
1	513	1	107	2.6
2	372	3	133	2.7
3	499	3	110	0.6
median of marketed CNS drugs <sup>a</sup>	305	1	45	2.8

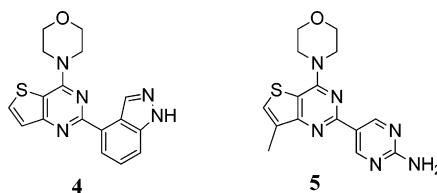
<sup>a</sup>Values reported are the median of 119 marketed CNS drugs as reported in ref 9.

the molecules could be reduced in size and TPSA while maintaining adequate potency. With an understanding of how the molecules bind to the enzyme from crystal structures with PI3K $\gamma$ , we decided that elimination of substitution at the 6-position of the thienopyrimidine core (numbering shown for 2 in Table 1) was least likely to have a dramatic impact on potency.<sup>4–6</sup> To that end, a comparison of 1 with 4 (Table 3) reveals that elimination of the benzylic piperazine sulfonamide group in 1 results in a 12-fold reduction in PI3K $\alpha$  potency and a corresponding reduction in cellular potency. On the other hand, a comparison of 2 and 3, which contain a 2-aminopyrimidine instead of the indazole of 1 with 5 shows that elimination of 6-position substitution results in a modest reduction in potency. That compound 5 maintained most of

the potency of 2 and 3 encouraged us that we could modulate the physicochemical properties of the thienopyrimidine molecules with a focus on the portion of the molecule exposed to solvent (6-position) without sacrificing potency.

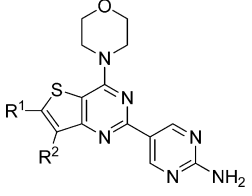
Importantly, Table 3 also reveals that truncating either 2 or 3 to the simple analogue 5 not only maintained potency but achieved a proof-of-concept that a reduction of transporter mediated efflux could be achieved in the thienopyrimidine series of PI3K inhibitors. On the other hand, a comparison of the human liver microsomal stability of 2 and 3 with 5 shows the importance of appropriate substitution of the 6-position for metabolic stability. To further illustrate this point, in vivo clearance of 5 in rats was well over the hepatic blood flow as compared to low clearance values for 2 and 3. Having identified 5 as a new suitable starting point for brain penetrant PI3K inhibitors we sought to further elucidate in silico correlations with transporter efflux and metabolic stability to guide selection of subsequent molecules for synthesis. We looked first for a correlation with transporter efflux, as this parameter was essential to our program.

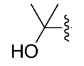
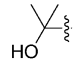
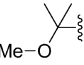
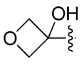
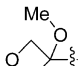
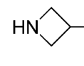
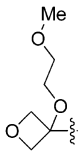
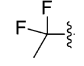
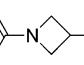
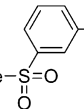
As 5 and 2 differ only by three heavy atoms but have very different Bcrp1 efflux ratios, the number of hydrogen bond donors appeared to play a significant role in the extent of efflux. To test this, we evaluated a number of analogues in permeability assays to elucidate the role of hydrogen bond donors in this series (Table 4). Compounds 2 and 6 have the

**Table 3.** A Comparison of the Potency, Permeability Efflux Ratios, in Vitro Metabolic Stability, and Rat CI of 1–3 with Analogues That Do Not Have Substitution in the Solvent Exposed Region (4 and 5)

compd	PI3K $\alpha$ IC <sub>50</sub> (nM)	PC3 proliferation EC <sub>50</sub> (nM)	B–A/A–B (MDR1)	B–A/A–B (Bcrp1)	human LM (mL/min/kg)	rat CI (mL/min/kg)
1	3	280	27	80	13	60
2	3	330	5	37	4	9
3	5	307	19	7	3	3
4	36	3600	4	1	16	nd
5	9	364	3	1	11	238

Table 4. Efflux Ratios and CNS MPO Scores for Select Thienopyrimidines



Compound	R <sup>1</sup>	R <sup>2</sup>	B-A/A-B (MDR1)	B-A/A-B (Bcrp1)	CNS MPO score
2		H	5.0	37	4.4
6		Me	3.9	5.4	4.3
7		H	0.9	3.7	4.8
8		Me	37	7.1	3.9
9		Me	1.8	1.3	4.5
10		H	37	22	3.7
11		H	1.6	1.4	4.0
12		H	0.9	1.7	5.0
13		H	44	43	4.4
14		Me	9	nd	3.6

same number of hydrogen bond donors, and both experience efflux with **6** having reduced Bcrp1 mediated efflux. However, compound **7**, which differs from **2** by a change of the tertiary alcohol to the corresponding methyl ether, has no efflux in the P-gp assay and moderate efflux in the Bcrp1 assay. Compounds **8** and **10** both contain R<sup>1</sup> groups with hydrogen bond donors and correspondingly are substrates of both P-gp and Bcrp1. The methyl ether compounds **9** and **11**, however, are not efflux transporter substrates. Compound **12** contains no ether but has the same HBD count as **5**, **7**, **9**, and **11** and is another example that is not a transporter substrate. Taken together, compounds **7**, **9**, **11**, and **12** confirmed the suspicion that hydrogen bond donor count plays a significant role in whether or not a compound in this series of molecules is a substrate of P-gp or Bcrp1. Confounding the simple analysis, however, are

compounds **13** and **14**, which are transporter substrates even though R<sup>1</sup> contains no HBD. Therefore, in an attempt to identify a better predictive measure of whether or not molecules in this series were likely to be transporter substrates, we attempted to find correlations between efflux and cLogP, TPSA, and MW. Unfortunately, we were unable to identify convincing trends (data not shown).

Recently, a central nervous system multiparameter optimization (CNS MPO) scoring system was reported as a holistic measure of the overall CNS drug-like properties of small molecules.<sup>10</sup> The CNS MPO algorithm assigns a score between 0 and 6 to a compound based on six calculated physicochemical properties (cLogP, cLogD, MW, TPSA, HBD, and pK<sub>a</sub>). One of the individual parameters contributing to this overall assessment of CNS drug-like attributes is P-gp mediated efflux

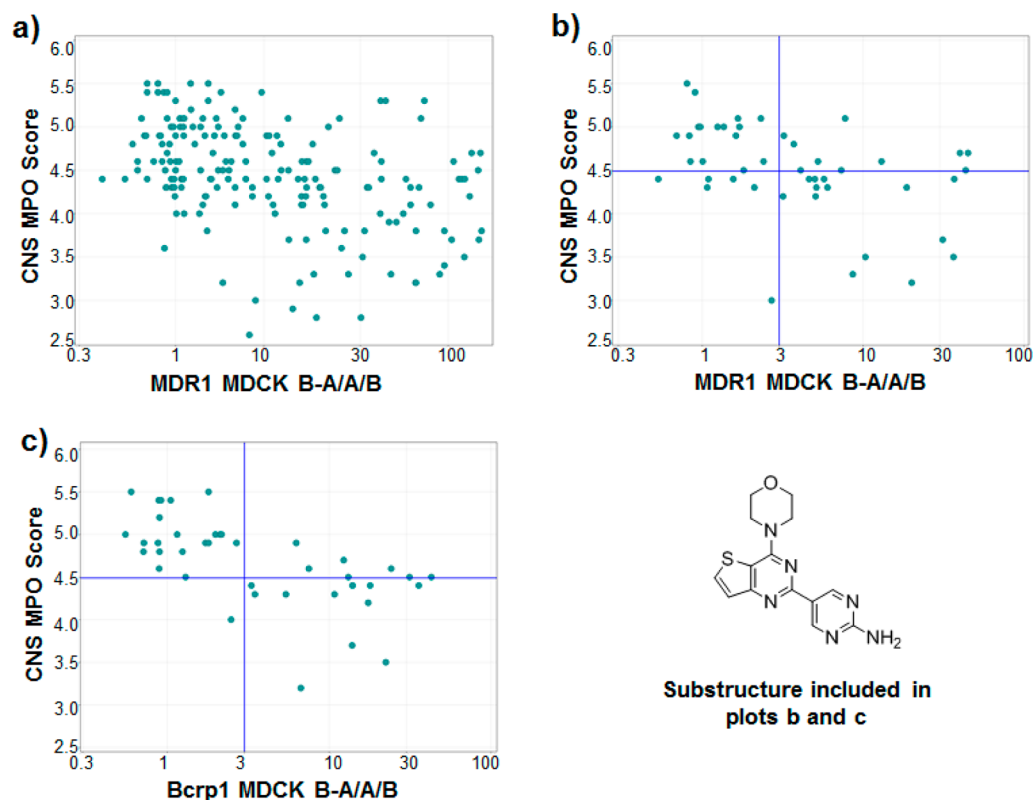


**Figure 1.** Plots of the relationship between transporter efflux and CNS MPO score. (a) The relationship of CNS MPO score and efflux for all PI3K inhibitors evaluated in our P-gp assay. (b) The relationship between CNS MPO score and P-gp efflux for molecules containing the thienopyrimidine substructure shown. (c) The relationship between CNS MPO score and Bcrp1 efflux for molecules containing the thienopyrimidine substructure shown.

and in the report of the CNS MPO scoring system a correlation between higher CNS MPO score and low P-gp efflux was shown.<sup>10,11</sup> We, therefore, sought to identify a correlation between CNS MPO score and likelihood of both P-gp and Bcrp1 mediated efflux within our own set of molecules. Figure 1a shows a correlative plot of CNS MPO score and P-gp efflux for all PI3K program molecules that were studied in the MDR1-MDCK permeability assay. In this plot, a general trend between higher CNS MPO score and low efflux is modest. When the data set is limited to thienopyrimidines substituted with an aminopyrimidine at the 2-position of the thienopyrimidine core, however, a correlation is seen (Figure 1b). Furthermore, a similar trend is observed when considering Bcrp1 mediated efflux (Figure 1c). On the basis of the apparent correlations between CNS MPO score and efflux, we prospectively turned our attention to only make or study molecules in this series that had a CNS MPO score  $\geq 4.5$ . At or above 4.5, 62% of molecules had low P-gp mediated efflux (B-A/A-B  $< 3$ ; 71% for Bcrp1) while those with a score  $< 4.5$  had a 16 in 20 chance of experiencing high P-gp efflux (13 of 14 for Bcrp1). It is worth noting that compounds 13 and 14 have CNS MPO scores of 4.4 and 3.6, respectively (Table 4), and so would have been expected to have a lesser chance of low efflux despite having the same number of hydrogen bond donors as 7, 9, and 12, which have scores of 4.8, 4.5, and 5.0, respectively.

The impact that the prospective use of CNS MPO evaluation had on the proportion of molecules made for the program that were transporter substrates is shown in Figure 2. Of the molecules made prior to implementing this *in silico* evaluation, 53% had high efflux mediated by P-gp and 66% by Bcrp1. After

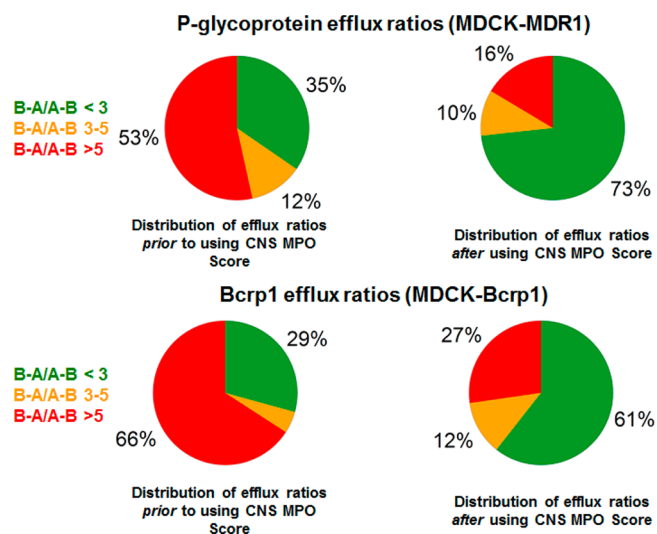
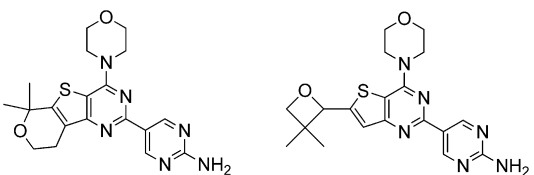


**Figure 2.** The distribution of efflux ratios experienced for molecules evaluated binned according to whether or not CNS MPO score was used as a prospective measure.

employing the CNS MPO score of  $\geq 4.5$  as a filter, new compounds were more than twice as likely as those made before using this filter to have low efflux as a result of either P-gp or Bcrp1 efflux.

The successful application of CNS MPO score to prioritize molecules likely to have low efflux lends additional support to the premise of a composite scoring system. Such a system is logical, with an appreciation that a particular physicochemical

Table 5. Physicochemical Properties of Thienopyrimidine PI3K Inhibitors That Have Low Efflux



compd	MW	HBD	TPSA	cLogP	CNS MPO score	B-A/A-B (MDR1)	B-A/A-B (Bcrp1)
7	386	2	99	2.4	4.8	0.9	3.7
9	414	2	108	1.0	4.5	1.8	1.3
15	398	2	99	2.1	4.9	1.0	2.3
16	398	2	99	2.1	4.9	1.9	1.2
median of marketed CNS drugs <sup>a</sup>	305	1	45	2.8			

<sup>a</sup>Values reported are the median of 119 marketed CNS drugs as reported in ref 9.

property value falling outside of a typical range for CNS drugs does not preclude that molecule from being a successful brain penetrant inhibitor. In our case, each of the molecules studied have a TPSA well above the median value of marketed CNS drugs and well above standard guidelines for CNS targeting agents (Table 5).<sup>12</sup> While the TPSA values are outside of the preferred range for even the CNS MPO score, the rest of the properties typically associated with BBB penetration, and included in the CNS MPO algorithm, are in a desirable range. That most properties are in the typical range associated with BBB penetration appears to compensate for the high TPSA and the composite of physicochemical properties are acceptable for low efflux.

Using CNS MPO, the majority of subsequently evaluated molecules for the program were not transporter substrates. As all compounds made also maintained the aminopyrimidine at the 2-position of the thienopyrimidine core, essentially every compound made also had acceptable biochemical and cellular potency (data not shown). What remained was to achieve compounds with desirable pharmacokinetic profiles in addition to low efflux. To that end, we employed an *in silico* evaluation of the likelihood of liver microsomal stability as a prospective assessment.<sup>13,14</sup> Our in-house model of liver microsomal stability employs a training set of more than 20000 historical molecules. The output of this model is a probability (0–1) of whether or not a compound will be stable or labile *in vitro* (stable:  $Cl_{hep} < 50\%$  liver blood flow; labile:  $Cl_{hep} > 50\%$  liver blood flow). Chemists prioritized molecules for synthesis that had a greater than 0.5 likelihood of being stable in human liver microsomes.<sup>15</sup>

We also identified a correlation between cLogP and the unbound clearance ( $Cl_u$ ) observed in rat *in vivo* studies (Figure 3). Within this series, molecules that had  $cLogP \leq 2.5$  had a

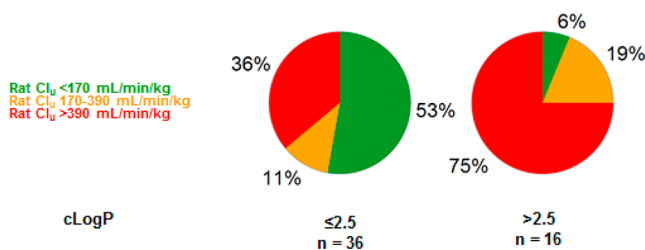


Figure 3. A comparison of Rat  $Cl_u$  for thienopyrimidine PI3K inhibitors binned according to cLogP.

greater likelihood of a low  $Cl_u$  in rats. Therefore, targeting molecules with cLogP under 2.5 would increase the likelihood that significant free drug exposure would be attained.

Having developed *in silico* correlations for efflux (HBD and CNS MPO) as well as metabolic stability (probability of human liver microsome stability and cLogP), a very narrow range of physicochemical properties was identified which would result in higher probability of low transporter efflux and acceptable pharmacokinetics. To demonstrate how few of our historical molecules fit into the range most likely to contain attractive brain penetrant PI3K inhibitors, Figure 4 shows all molecules

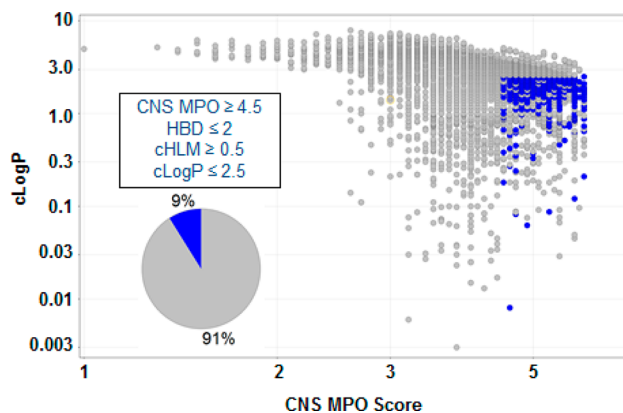


Figure 4. A display of all compounds made for Genentech PI3K programs binned according to whether they fit (blue) or do not fit (gray) each of the criteria for thienopyrimidine PI3K inhibitors deemed most likely to result in brain penetration and desirable pharmacokinetic properties.

made for our PI3K programs (targeting systemic circulation only as well as brain penetrant molecules). Of all the molecules synthesized, 9% fit into the targeted space. The identification of such a narrow target space allowed for careful selection of a small number of molecules for synthesis and resulted in rapid identification of attractive brain penetrant PI3K inhibitors.

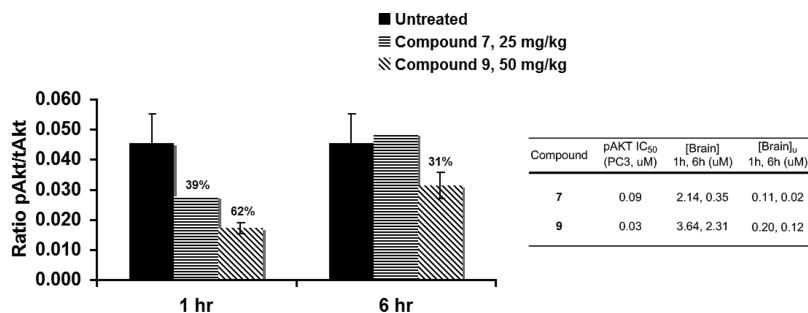
After evaluating efflux *in vitro*, several compounds that fit the preferred criteria were studied in mice to evaluate their pharmacokinetic profile as well as to confirm brain penetration (Table 6). Each of the compounds in Table 6 had acceptable clearance in mice, with **16** having the highest clearance of the group. As expected based on their low *in vitro* efflux, **7**, **9**, **15**, and **16** each achieve significant penetration of the BBB as



Table 6. Potency, Efflux Ratios, Mouse PK, and Brain Exposure for Select Molecules<sup>a</sup>

compd	PI3K- $\alpha$ K <sub>i,app</sub> (nM)	mTOR K <sub>i,app</sub> (nM)	Pc3 proliferation EC <sub>50</sub> (nM)	B-A/A-B (MDR1)	B-A/A-B (Bcrp1)	mouse CI (mL/min/kg)	mouse t <sub>1/2</sub> (h)	mouse F%	mouse PPBd (%)	[Brain]/ [Plasma] (1 h, 6 h)	[Brain] <sub>u</sub> / [Plasma] <sub>u</sub> (1 h, 6 h)
2	3	30	330	5	3.7	17	2.2	100	80.2	0.3, 0.2 <sup>b</sup>	0.04, nd <sup>b</sup>
7	1	10	170	1.6	1.0	20	20	25	89.8	1.0, 0.9 <sup>c</sup>	0.5, 0.4 <sup>c</sup>
9	2	9	132	1.5	1.3	32	17	75	85.0	1.0, 1.0 <sup>d</sup>	0.4, 0.4 <sup>d</sup>
15	1	13	215	0.8	2.3	16	2.9	93	99.4	1.4, 1.6 <sup>e</sup>	0.7, 0.8 <sup>e</sup>
16	1	21	185	1.9	1.2	52	3.3	46	91.3	0.9, 1.2 <sup>c</sup>	0.3, 0.3 <sup>c</sup>

<sup>a</sup>All [Brain]/[Plasma] ratios determined after oral dose of female nu/nu mice with the indicated compound as an MCT suspension. t<sub>1/2</sub> is reported for the oral dose. <sup>b</sup>Determined after administration of 15 mg/kg and [Brain]/[Plasma] determined at 0.5 and 4 h. <sup>c</sup>Determined after administration of 25 mg/kg. <sup>d</sup>Determined after administration of 50 mg/kg. <sup>e</sup>Determined after administration of 15 mg/kg.



**Figure 5.** Inhibition of pAKT in female CD-1 mice after oral administration of 7 and 9 as MCT suspension. Normalized pAKT was measured 1 and 6 h post dose and are indicated by the bars in the chart, and error bars indicate  $\pm$  standard error of the mean. The percentage reduction in pAKT compared to the untreated group is indicated where applicable. The mean pAKT for the untreated groups are based on samplings of brain tissue from three animals per time point. Sampling of one animal per time point was analyzed for compound 7.

measured by brain-to-plasma ratios and free concentration in the brain relative to free plasma concentrations. While 15 achieved the highest unbound brain-to-plasma ratio, the high protein binding in the mouse (99.4% plasma, 99.7% brain) limited the free concentration achieved in the brain (9 and 13 nM at 1 and 6 h, respectively). Furthermore, compounds 7 and 9 had the longest t<sub>1/2</sub> of this set of molecules. Each of these selected molecules potently inhibits both PI3K- $\alpha$  and mTOR and has good potency in an antiproliferation cell assay using PC3 cells. In addition, each of these compounds inhibits each of the class I PI3K isoforms (available in Supporting Information). Compounds 7 and 9, selected for further study below, were evaluated in a panel of 59 kinases (excluding class I PI3Ks) provided by Invitrogen's SelectScreen service. Only 9 inhibited any kinase in the panel by >75% at 1  $\mu$ M concentration of the test compound (PI3KC2 $\beta$ , 77%).

On the basis of the results in Table 6, and to further demonstrate the value of these brain penetrant inhibitors, compounds 7 and 9 were selected to demonstrate inhibition of PI3K signaling through AKT behind the BBB. To this end, we measured the ratio of pAKT to total AKT in normal brain tissue in mice treated with 7 or 9 (Figure 5). Oral administration of 7 and 9 (25 and 50 mg/kg, respectively) each resulted in significant inhibition of pAKT at the 1 h time point. Compound 9 continued to inhibit pAKT 6 h post dose, perhaps differentiating from 7 because of the higher dose studied. These results are consistent with the free brain concentrations measured at those time points and the pAKT IC<sub>50</sub> (PC3 cell line) determined for each of the compounds (Figure 5). These experiments demonstrate that the molecules significantly inhibit their target beyond the BBB in normal mice and contrast with results obtained with administration of our clinical inhibitors of PI3K 1 and 3, which do not inhibit pAKT in normal mice brains.<sup>8,16</sup>

To evaluate the potential general applicability of a PI3K inhibitor in GBM, we studied 7 and 9 in a panel of glioblastoma cell lines (Table 7). In six of the seven lines tested, both 7 and 9

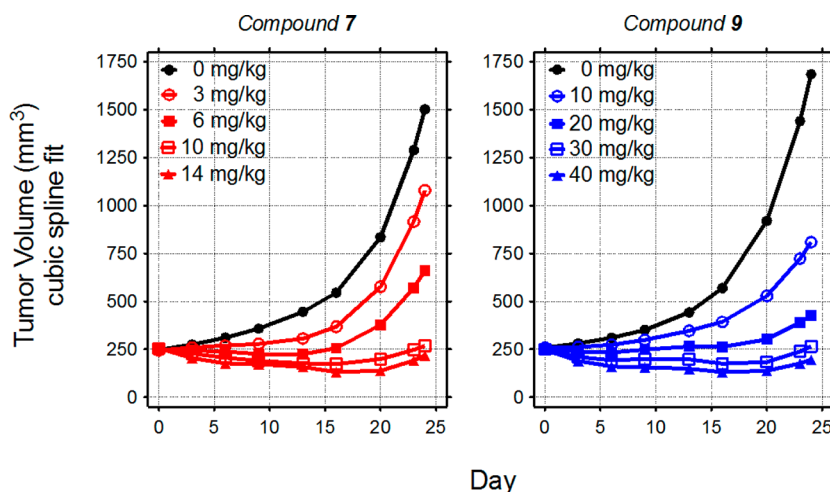
**Table 7.** Antiproliferative EC<sub>50</sub>'s for 7 and 9 in a Panel of Seven Glioblastoma Cell Lines

cell line	7 proliferation EC <sub>50</sub> ( $\mu$ M)	9 proliferation EC <sub>50</sub> ( $\mu$ M)
A172	0.38	0.24
HS683	0.27	0.23
LN-229	0.40	0.14
MO59J	0.59	0.33
SF539	0.34	0.25
U87-MG-Luc	0.29	0.25
SF268	1.0	0.57

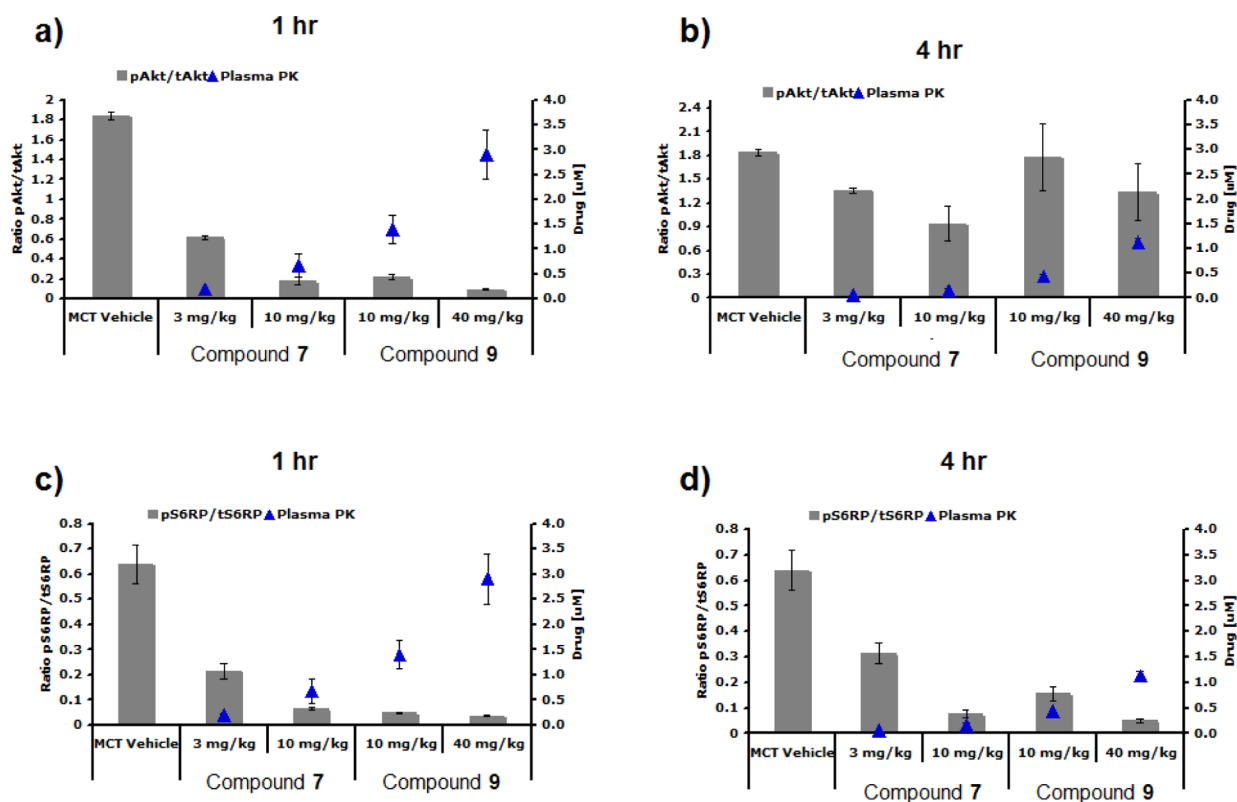
had antiproliferative EC<sub>50</sub>s < 600 nM. The SF268 line was more weakly affected and, along with the LN-229 line, is one of two cell lines studied not deficient for PTEN.

To demonstrate the inhibition of tumor growth in a GBM model, compounds 7 and 9 were studied in a U87 subcutaneous xenograft study (Figure 6). The daily oral administration of 7 and 9 to female NCr nude mice bearing subcutaneous U-87 MG/M human glioblastoma xenografts resulted in dose-dependent inhibition of tumor growth. Inhibition of tumor growth by 7 was first observed at 3 mg/kg, while 6 mg/kg resulted in tumor stasis for most of the dosing period and doses  $\geq$ 10 mg/kg caused regression. Administration of 9 began negatively affecting the growth of such xenografts at 10 mg/kg, resulted in tumor stasis at 20 mg/kg for most of the 24-day dosing period, and regressed tumors at doses  $\geq$ 30 mg/kg.

The general tolerability of once daily dosing of 7 and 9 was assessed by the percentage change in body weights.<sup>17</sup>



**Figure 6.** In vivo efficacy of 7 and 9 versus U87 MG/M human glioblastoma xenografts. Female NCr nude mice bearing subcutaneous tumors were administered escalating doses of 7 or 9 orally as a suspension in vehicle (0.5% methylcellulose/0.2% Tween-80) or vehicle once daily (QD) for 24 days. Changes in tumor volumes over time by dose for each compound are depicted as cubic spline fits generated via linear mixed effects analysis of log-transformed volumes.

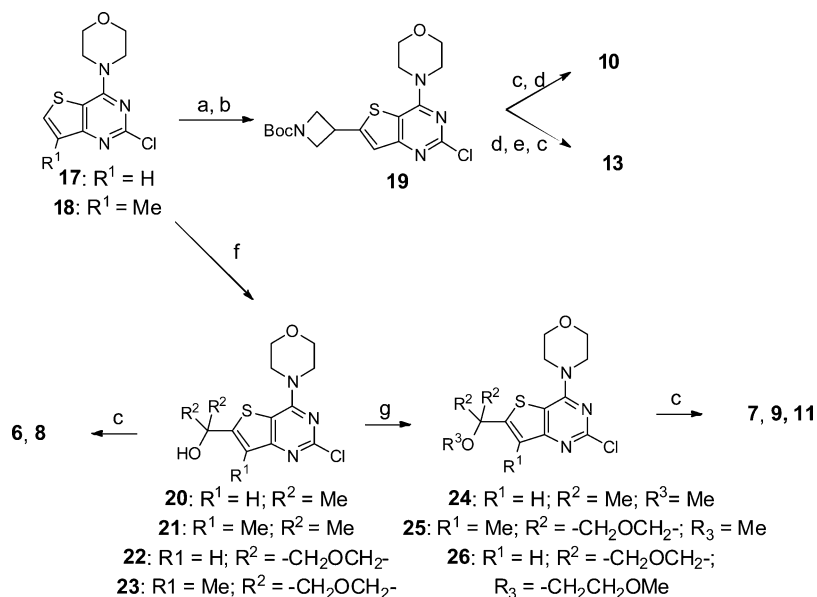


**Figure 7.** Effect of 7 and 9 on PD markers in the U87 MG/M human glioblastoma xenograft model after 24 days of continuous dosing. Tumors were excised from animals 1 and 4 h after the last administered dose on day 24 and processed for analysis of PI3K/Akt pathway markers as described in the Experimental Section. Indicated values are the means for groups of three animals, and error bars indicate  $\pm$  standard error of the mean. (a,b) Levels of pAkt (Ser473) and total Akt were measured by electrochemiluminescence using Meso Scale Discovery (Gaithersburg, MD) according to manufacturer's instructions. (c,d) pS6RP(Ser235/236) and total S6RP were assessed using assays measuring electrochemiluminescence from Meso Scale Discovery according to manufacturer's instructions.

Compound 7 did not cause body weight loss up to 6 mg/kg, resulted in body weight loss of <15% in the majority of the animals at 14 mg/kg, and was not tolerated at 18 mg/kg. Compound 9 was well tolerated up to 30 mg/kg, caused <15% body weight loss at 40 mg/kg, and resulted body weight loss in excess of 15% in the majority of the animals at 50 mg/kg. On the basis of these observations, 14 and 40 mg/kg were deemed

the maximum tolerated dose of 7 and 9 when administered orally once daily, respectively. At such doses, the tumor growth inhibition was near maximal for both compounds.

Additionally, the tumor growth inhibition achieved by 7 and 9 came with a corresponding inhibition of pAKT and pS6RP (Figure 7). The inhibition of these downstream markers is a strong indicator that the tumor growth inhibition is the result

Scheme 1<sup>a</sup>

<sup>a</sup>Reagents and conditions: (a) 2.5 M *n*-BuLi, THF; I<sub>2</sub>; (b) Zn, CH<sub>3</sub>SiCl, 3-iodoazetidine-1-*t*-butylcarboxylate, BrCH<sub>2</sub>CH<sub>2</sub>Br, DMA; Pd(dppf)Cl<sub>2</sub>, CuI; (c) 2-aminopyrimidine-5-boronic acid pinacol ester, PdCl<sub>2</sub>(PPh<sub>3</sub>)<sub>2</sub>, 1 M aq KOAc, CH<sub>3</sub>CN, microwave, 150 °C, 15 min; (d) TFA, CH<sub>2</sub>Cl<sub>2</sub>; (e) Ac<sub>2</sub>O, Et<sub>3</sub>N, CH<sub>2</sub>Cl<sub>2</sub>; (f) 2.5 M *n*-BuLi, THF; ketone; (g) NaH, alkyl iodide, DMF.

of on-target inhibition. Furthermore, 1 h after dosing mice with **9** in the U87 subcutaneous xenograft study with the efficacious dose of 40 mg/kg, the concentration achieved in tumor is still less than that achieved in healthy mouse brains after a 50 mg/kg dose (2.2 and 3.6 μM, respectively). That efficacy is achieved in a subcutaneous xenograft model where tumor concentration is less than that achieved in the brain lends additional encouragement to the use of **9** for the treatment of GBM.

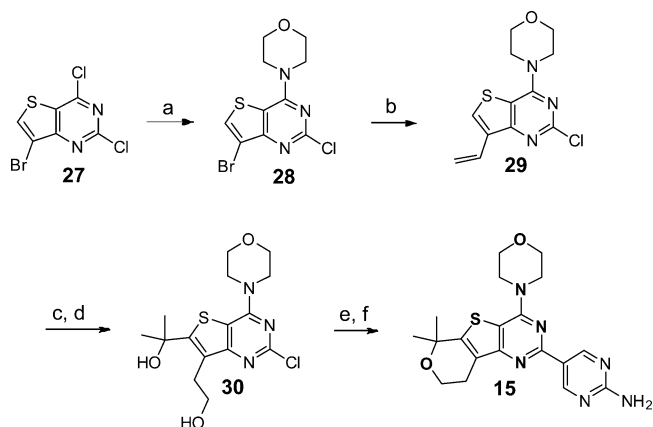
## CHEMISTRY

A representative synthesis of compounds **4–14** (Scheme 1) commenced with the appropriate morpholinopyrimidine (**17**<sup>5</sup> or **18**<sup>6</sup>).<sup>18</sup> Lithiation of thiophene **17** followed by trapping with iodine, subsequent Negishi coupling, and Boc deprotection afforded azetidines **19**. Suzuki coupling provided compound **10**, and subsequent acetylation provided **13**. Alternatively, the lithiated thiophene can be trapped with either acetone or oxetanone to yield **20–23**. The tertiary alcohol intermediates were used in Suzuki couplings to provide final compounds (**6, 8**) or converted to ethers prior to Suzuki coupling that yielded **7, 9**, and **11**.

The synthesis of **15** began with incorporation of morpholine onto dichloropyrimidine **27**<sup>19</sup> to produce **28** (Scheme 2). Stille coupling of bromothiophene **28** afforded **29**. Hydroboration and subsequent oxidation of the vinyl group followed by lithiation of the thiophene followed by trapping with acetone resulted in a diol that was immediately cyclized under acidic conditions to yield **30**. Finally, Suzuki coupling resulted in the final product **15**.

## CONCLUSION

Herein we have described the successful realization of property guided design of brain penetrant inhibitors of PI3K. Several in silico measures were used to prospectively select compounds for synthesis and evaluation likely to have low efflux and good metabolic stability. After confirming low efflux in vitro and

Scheme 2<sup>a</sup>

<sup>a</sup>Reagents and conditions: (a) morpholine, MeOH; (b) *n*-Bu<sub>3</sub>SnCH<sub>2</sub>CH<sub>2</sub>, Pd(PPh<sub>3</sub>)<sub>4</sub>, 1,4-dioxane; (c) 9-BBN, THF; 20 M aq H<sub>2</sub>O<sub>2</sub>, 5 M aq NaOH; (d) 2.5 M *n*-BuLi, THF; acetone; (e) TFA, toluene; (f) 2-aminopyrimidine-5-boronic acid pinacol ester, PdCl<sub>2</sub>(PPh<sub>3</sub>)<sub>2</sub>, 1 M aq KOAc, CH<sub>3</sub>CN, microwave, 150 °C, 15 min.

good brain exposure, compounds **7** and **9** demonstrated pathway inhibition in normal brain tissue, inhibition of tumor growth in the U87 model of glioblastoma, and good potency in a panel of GBM cell lines. Given the significant role that the PI3K pathway plays in glioblastoma, brain penetrant PI3K inhibitors have the potential to address a significant unmet medical need. Given the frequent association of aberrant signaling of the PI3K pathway in GBM, and our molecules' ability to inhibit PI3K signaling beyond the BBB, we are continuing our study of these and other molecules for clinical application. Studies of **9** in additional GBM models will be reported elsewhere.<sup>20</sup>



## EXPERIMENTAL SECTION

**Chemistry.** All solvents and reagents were used as obtained.  $^1\text{H}$  NMR spectra were recorded with a Bruker Avance DPX400 spectrometer or a Varian Inova 400 NMR spectrometer and referenced to tetramethyl silane. chemical shifts are expressed as  $\delta$  units using tetramethylsilane as the external standard (in NMR description: s, singlet; d, doublet; t, triplet; q, quartet; m, multiplet; br, broad peak). All final compounds were purified to >95% chemical purity, as assayed by HPLC (Waters Acquity UPLC column, 21 mm  $\times$  50 mm, 1.7  $\mu\text{m}$ ) with a gradient of 0–90% acetonitrile (containing 0.038% TFA) in 0.1% aqueous TFA, with UV detection at  $\lambda = 254$  and 210 nm, and with CAD detection with an ESA Corona detector.

1–4 have been described previously.<sup>4–6</sup>

**5-(7-Methyl-4-morpholinothieno[3,2-*d*]pyrimidin-2-yl)pyrimidin-2-amine (5).** A mixture of 4-(2-chloro-7-methylthieno[3,2-*d*]pyrimidin-4-yl)morpholine (**18**)<sup>6</sup> (172.9 mg, 0.641 mmol), 5-(4,4,5,5-tetramethyl-1,3,2-dioxaborolan-2-yl)pyrimidin-2-amine (109 mg, 0.493 mmol), bis(ditert-butyl(4-dimethylaminophenyl)phosphine) dichloropalladium(II) (36.0 mg, 0.049 mmol), and 1 M  $\text{Na}_2\text{CO}_3$  (2.0 mL) in acetonitrile (2 mL) was purged with nitrogen for 1 min in a microwave vial. The vessel was sealed and heated to 130 °C for 20 min in a Biotage Initiator microwave. Upon cooling, the aqueous layer was removed and the organic layer was concentrated under reduced pressure. The residue was purified by HPLC to give **5** (94 mg, 58% yield).  $^1\text{H}$  NMR (400 MHz,  $\text{DMSO-}d_6$ )  $\delta$  9.17 (s, 2H), 7.86 (d,  $J = 1.3$  Hz, 1H), 7.06 (s, 2H), 3.97 (t,  $J = 4.7$  Hz, 4H), 3.78 (t,  $J = 4.8$  Hz, 4H), 2.40 (d,  $J = 1.0$  Hz, 3H). LCMS (ESI):  $m/z = 329.1$  [ $\text{M} = \text{H}$ ]<sup>+</sup>.

**2-(2-Chloro-7-methyl-4-morpholinothieno[3,2-*d*]pyrimidin-6-yl)propan-2-ol (21).** *n*-Butyllithium (2.5 M) in hexanes (3.9 mL, 9.6 mmol) was added to **18**<sup>6</sup> (2.0 g, 7.4 mmol) in THF (60 mL) at –48 °C under nitrogen and the reaction stirred 30 min. Added anhydrous acetone (2.2 mL, 30 mmol) and stirred 30 min at –48 °C. The reaction was quenched with water and extracted with EtOAc. The combined organics were dried over  $\text{MgSO}_4$ , filtered, and concentrated under reduced pressure to give 2-(2-amino-7-methyl-4-morpholinothieno[3,2-*d*]pyrimidin-6-yl)propan-2-ol (1.9 g, 80% yield).  $^1\text{H}$  NMR (400 MHz,  $\text{DMSO-}d_6$ )  $\delta$  3.97–3.85 (m, 4H), 3.75 (q,  $J = 4.3$  Hz, 4H), 2.32 (s, 3H), 1.58 (s, 6H). LCMS (ESI):  $m/z = 328.4$  [ $\text{M} = \text{H}$ ]<sup>+</sup>.

**2-(2-(2-Aminopyrimidin-5-yl)-7-methyl-4-morpholinothieno[3,2-*d*]pyrimidin-6-yl)propan-2-ol (6).** A mixture of **21** (250 mg, 0.76 mmol), 5-(4,4,5,5-tetramethyl-1,3,2-dioxaborolan-2-yl)pyrimidin-2-amine (200 mg, 0.92 mmol), tetrakis(triphenylphosphine)palladium(0) (44.0 mg, 0.038 mmol), and 1 M  $\text{Na}_2\text{CO}_3$  (2.0 mL) in acetonitrile (2 mL) was purged with nitrogen for 1 min in a microwave vial. The vessel was sealed and heated to 140 °C for 20 min in a Biotage Initiator microwave. Upon cooling, the aqueous layer was removed and the organic layer was concentrated under reduced pressure. The residue was purified by HPLC to give **6** (23 mg, 8% yield).  $^1\text{H}$  NMR (400 MHz,  $\text{DMSO-}d_6$ )  $\delta$  9.16 (s, 2H), 7.06 (s, 1H), 7.06 (s, 2H), 3.97 (t,  $J = 4.7$  Hz, 4H), 3.78 (t,  $J = 4.8$  Hz, 4H), 2.45 (s, 3H), 1.60 (s, 6H). LCMS (ESI):  $m/z = 387.1$  [ $\text{M} = \text{H}$ ]<sup>+</sup>.

**4-(2-Chloro-6-(2-methoxypropan-2-yl)thieno[3,2-*d*]pyrimidin-4-yl)morpholine (24).** 2-(2-Chloro-4-morpholinothieno[3,2-*d*]pyrimidin-6-yl)propan-2-ol (**20**)<sup>5</sup> (0.25 g, 0.8 mmol) was dissolved in dimethylformamide (5 mL) and cooled to 0 °C under nitrogen. Sodium hydride (23 mg, 0.9 mmol) was added, and the reaction mixture was stirred for 10 min. Methyl iodide (0.1 mL, 1.2 mmol) was added and the reaction was allowed to warm to room temperature and stirred for 1 h. The reaction was quenched with saturated aqueous  $\text{NaHCO}_3$  and extracted with EtOAc to give **24** (260 mg, 96% yield).  $^1\text{H}$  NMR (400 MHz,  $\text{CDCl}_3$ )  $\delta$  5.03–4.93 (m, 4H), 4.01 (t,  $J = 5.6$ , 4.1 Hz, 4H), 3.85 (m, 4H), 3.18 (s, 3H), 2.37 (s, 3H). LCMS (ESI):  $m/z = 328.3$  [ $\text{M} = \text{H}$ ]<sup>+</sup>.

**5-(6-(2-Methoxypropan-2-yl)-4-morpholinothieno[3,2-*d*]pyrimidin-2-yl)pyrimidin-2-amine (7).** **24** (0.25 g, 0.76 mmol), 5-(4,4,5,5-tetramethyl-1,3,2-dioxaborolan-2-yl)pyrimidin-2-amine (200 mg, 0.92 mmol), tetrakis(triphenylphosphine)palladium(0) (44.0 mg, 0.038 mmol), and 1 M aqueous  $\text{Na}_2\text{CO}_3$  (2.0 mL) was combined in

acetonitrile (2 mL) and purged with nitrogen for 1 min in a microwave vial. The vessel was sealed and heated to 140 °C for 20 min in a Biotage Initiator microwave. Upon cooling, the aqueous layer was removed and the organic layer was concentrated under reduced pressure. The residue was purified by HPLC to give **7** (49 mg, 17% yield).  $^1\text{H}$  NMR (400 MHz,  $\text{DMSO-}d_6$ )  $\delta$  9.11 (s, 2H), 7.35 (s, 1H), 7.04 (s, 2H), 3.96 (t,  $J = 4.7$  Hz, 4H), 3.78 (t,  $J = 4.8$  Hz, 4H), 3.14 (s, 3H), 1.61 (s, 6H). LCMS (ESI):  $m/z = 387.1$  [ $\text{M} = \text{H}$ ]<sup>+</sup>.

**3-2-Chloro-7-methyl-4-morpholinothieno[3,2-*d*]pyrimidin-6-yl)oxetan-3-ol (23).** **18**<sup>6</sup> (15 g, 56 mmol) was dissolved in THF (500 mL) and cooled to –48 °C under nitrogen. *n*-Butyllithium (2.5 M) was added in hexanes (29 mL, 72 mmol) and stirred for 30 min. 3-Oxetanone (16 g, 220 mmol) was added and stirred for 30 min at –48 °C. The reaction was quenched with water and extracted with EtOAc, dried over  $\text{MgSO}_4$ , filtered, and concentrated under reduced pressure to give **23** (10.6 g, 56% yield).  $^1\text{H}$  NMR (400 MHz,  $\text{DMSO-}d_6$ )  $\delta$  7.10 (s, 2H), 4.95 (d,  $J = 7.0$  Hz, 2H), 4.86 (d,  $J = 7.0$  Hz, 2H), 3.90 (t,  $J = 4.8$  Hz, 4H), 3.74 (t,  $J = 4.8$  Hz, 4H), 2.43 (s, 2H). LCMS (ESI):  $m/z = 342.2$  [ $\text{M} = \text{H}$ ]<sup>+</sup>.

**3-(2-(2-Aminopyrimidin-5-yl)-7-methyl-4-morpholinothieno[3,2-*d*]pyrimidin-6-yl)oxetan-3-ol (8).** **23** (0.26 g, 0.76 mmol), 5-(4,4,5,5-tetramethyl-1,3,2-dioxaborolan-2-yl)pyrimidin-2-amine (200 mg, 0.92 mmol), tetrakis(triphenylphosphine)palladium(0) (44.0 mg, 0.038 mmol), and 1 M  $\text{Na}_2\text{CO}_3$  (2.0 mL) were combined in acetonitrile (2 mL) and purged with nitrogen for 1 min in a microwave vial. The vessel was sealed and heated to 140 °C for 20 min in a Biotage Initiator microwave. Upon cooling, the aqueous layer was removed and the organic layer was concentrated under reduced pressure. The residue was purified by HPLC to give **8** (77 mg, 25% yield).  $^1\text{H}$  NMR (400 MHz,  $\text{DMSO-}d_6$ )  $\delta$  9.16 (s, 2H), 7.08 (s, 2H), 5.19–5.12 (m, 4H), 3.95 (t,  $J = 4.7$  Hz, 4H), 3.71 (t,  $J = 4.8$  Hz, 4H), 2.44 (s, 3H). LCMS (ESI):  $m/z = 401.1$  [ $\text{M} = \text{H}$ ]<sup>+</sup>.

**4-(2-Chloro-6-(3-methoxyoxetan-3-yl)-7-methylthieno[3,2-*d*]pyrimidin-4-yl)morpholine (25).** **23** (0.5 g, 2.0 mmol) was dissolved in DMF (5 mL, 60 mmol) and cooled to 0 °C. Sodium hydride (73 mg, 3.0 mmol) was added and stirred for 10 min. Methyl iodide (0.24 mL, 3.8 mmol) was added and allowed to warm to room temperature and stirred 1 h. The reaction was quenched with saturated aqueous  $\text{NaHCO}_3$  and extracted with EtOAc, dried over  $\text{MgSO}_4$ , filtered, and concentrated under reduced pressure. The crude material was purified by silica gel chromatography (0–50% EtOAc in heptane) to give **25** (0.45 mg, 98% yield).  $^1\text{H}$  NMR (400 MHz,  $\text{CDCl}_3$ ) 5.03–4.93 (m, 4H), 4.01 (t,  $J = 4.9$  Hz, 4H), 3.85 (t,  $J = 4.8$  Hz, 4H), 3.18 (s, 3H), 2.37 (s, 3H). LCMS (ESI):  $m/z = 356.0$  [ $\text{M} = \text{H}$ ]<sup>+</sup>.

**5-(6-(3-Methoxyoxetan-3-yl)-7-methyl-4-morpholinothieno[3,2-*d*]pyrimidin-2-yl)pyrimidin-2-amine (9).** **25** (0.27 g, 0.76 mmol), 5-(4,4,5,5-tetramethyl-1,3,2-dioxaborolan-2-yl)pyrimidin-2-amine (200 mg, 0.92 mmol), tetrakis(triphenylphosphine)palladium(0) (44.0 mg, 0.038 mmol), and 1 M  $\text{Na}_2\text{CO}_3$  (2.0 mL) were combined in acetonitrile (2 mL) and purged with nitrogen for 1 min in a microwave vial. The vessel was sealed and heated to 140 °C for 20 min in a Biotage Initiator microwave. Upon cooling, the aqueous layer was removed and the organic layer was concentrated under reduced pressure. The residue was purified by HPLC to give **9** (48 mg, 15% yield).  $^1\text{H}$  NMR (400 MHz,  $\text{DMSO-}d_6$ )  $\delta$  9.17 (s, 2H), 7.08 (s, 2H), 4.97–4.87 (m, 4H), 3.98 (t,  $J = 5.0$  Hz, 4H), 3.79 (t,  $J = 4.8$  Hz, 4H), 3.13 (s, 3H), 2.34 (s, 2H). LCMS (ESI):  $m/z = 415.1$  [ $\text{M} = \text{H}$ ]<sup>+</sup>.

**tert-Butyl 3-(2-Chloro-4-morpholinothieno[3,2-*d*]pyrimidin-6-yl)azetidine-1-carboxylate (19).** To a mixture of zinc (1.4 g, 0.02 mol) in degassed DMA under nitrogen was added chlorotrimethylsilane (0.2 mL, 0.002 mol) and dibromoethane (0.12 mL, 0.0014 mol). The mixture was stirred for 15 min, and *tert*-butyl 3-iodoazetidine-1-carboxylate (4 g, 0.01 mol) in degassed DMA was added slowly. The resulting solution was stirred at room temperature for 1.5 h to form (1-(*tert*-butoxycarbonyl)azetidin-3-yl)zinc(II) iodide. 4-(2-Chloro-6-iodothieno[3,2-*d*]pyrimidin-4-yl)morpholine<sup>21</sup> (1.52 g, 3.98 mol) was dissolved in DMA (7 mL) and degassed for 5 min,  $\text{Pd}(\text{dppf})\text{Cl}_2$  (163 mg, 0.2 mmol) and  $\text{CuI}$  (75 mg, 0.398 mmol) were added, and the

reaction followed by the previously generated solution of (1-(*tert*-butoxycarbonyl)azetidin-3-yl)zinc(II) iodide. The reaction was heated to 80 °C for 1 h. The reaction mixture was partitioned between 1 N HCl and EtOAc. The aqueous phase was basified to pH 13 with 1 N NaOH. The aqueous phase was filtered and rinsed with cold water to afford **19** as white solid (1.1 g, 70% yield). <sup>1</sup>H NMR (400 MHz, CDCl<sub>3</sub>) δ 7.20–7.12 (s, 1H), 4.47–4.34 (m, 2H), 4.12–4.02 (m, 3H), 4.02–3.92 (t, *J* = 4.9 Hz, 4H), 3.92–3.78 (t, *J* = 4.8 Hz, 4H), 1.50–1.45 (s, 9H). LC/MS (ESI+): *m/z* 411.0 (M + H).

**5-(6-(Azetidin-3-yl)-4-morpholinothieno[3,2-*d*]pyrimidin-2-yl)pyrimidin-2-amine (10).** To a microwave vial was added *tert*-butyl 3-(2-chloro-4-morpholinothieno[3,2-*d*]pyrimidin-6-yl)azetidyl-1-carboxylate (60 mg, 1.0 mmol), 2-aminopyrimidine-5-boronic acid, and pinacol ester (48 mg, 0.2 mmol) 1 M cesium carbonate solution in water (0.44 mL, 0.44 mmol) followed by 1,1'-bis(diphenylphosphino)ferrocene-palladium(II) chloride (20 mg, 0.03 mmol). The mixture was degassed under nitrogen for 5 min, then subjected to microwave irradiation at 140 °C for 30 min. The crude mixture was filtered through a thin layer of Celite, and the filtered organics were diluted with EtOAc and washed with water. The organic layer was concentrated under reduced pressure and partially purified by silica gel chromatography LC/MS (ESI+): *m/z* 470.2 (M + H). The partially purified intermediate (60 mg, 1.0 mol) was treated with TFA (1 mL) in CH<sub>2</sub>Cl<sub>2</sub> (1 mL), and stirred 1 h. Saturated aqueous NaHCO<sub>3</sub> was added, and the aqueous layer was extracted with 10% MeOH/EtOAc, dried over MgSO<sub>4</sub>, filtered, and concentrated to give **10** after HPLC purification (31 mg, 59% yield over two steps). <sup>1</sup>H NMR (400 MHz, DMSO) δ 9.18–9.02 (s, 2H), 7.63–7.45 (s, 1H), 7.18–6.96 (s, 2H), 4.44–4.30 (p, *J* = 8.0 Hz, 1H), 4.31–4.18 (t, *J* = 9.1 Hz, 2H), 4.11–4.00 (dd, *J* = 9.8, 7.4 Hz, 2H), 4.00–3.90 (t, *J* = 4.7 Hz, 4H), 3.85–3.72 (t, *J* = 4.7 Hz, 4H). LC/MS (ESI+): *m/z* 370.1 (M + H).

**3-(2-Chloro-4-morpholinothieno[3,2-*d*]pyrimidin-6-yl)-oxetan-3-ol (22).** To a solution of **17** (1.9 g, 7.4 mmol) in THF (60 mL) at –48 °C was added 2.5 M of *n*-butyllithium in hexane (3.9 mL, 9.6 mmol) and the reaction stirred for 30 min. 3-Oxetanone (2.1 mL, 3.0 mmol) was added and the reaction stirred another 30 min. The reaction was quenched by slowly transferring the still cool reaction slurry into a large Erlenmeyer flask containing ice and 2 N aqueous HCl. This reaction mixture was stirred for several minutes prior to transfer to a separatory funnel. The reaction mixture was extracted with three portions of EtOAc. The combined organics were dried over Na<sub>2</sub>SO<sub>4</sub> and concentrated. The crude material was purified by silica gel chromatography eluting with 0–50% EtOAc in DCM to give **22** (2.0 g, 82% yield). <sup>1</sup>H NMR (400 MHz, DMSO) δ 7.19 (s, 1H), 4.79 (q, *J* = 6.7 Hz, 4H), 3.90 (t, *J* = 4.8 Hz, 5H), 3.75 (dd, *J* = 5.7, 3.8 Hz, 5H). LCMS (ESI): *m/z* = 328.0 [M + H]<sup>+</sup>.

**4-(2-Chloro-6-(3-(2-methoxyethoxy)oxetan-3-yl)thieno[3,2-*d*]pyrimidin-4-yl)morpholine (26).** To an ice-cooled solution of 3-(2-chloro-4-morpholinothieno[3,2-*d*]pyrimidin-6-yl)oxetan-3-ol (1.26 g, 3.84 mmol) in *N,N*-dimethylformamide (11.9 mL, 154 mmol) was added portionwise sodium hydride (184 mg, 7.7 mmol). The reaction mixture was stirred for 10 min, followed by the addition of 1-bromo-2-methoxyethane (0.9 mL, 9.6 mmol). The cooling bath was allowed to dissipate and the reaction mixture stirred 90 min. The reaction mixture was cooled to 0 °C and quenched by portionwise addition of ice chips and cold water. The quenched reaction was transferred to a separatory funnel, and the aqueous layer was extracted with three portions of EtOAc. The combined organics were dried over Na<sub>2</sub>SO<sub>4</sub>, filtered, and concentrated. This crude material was purified by silica gel chromatography (10–50% EtOAc/heptane) to give **26** (900 mg, 60% yield). <sup>1</sup>H NMR (400 MHz, DMSO) δ 7.20 (s, 1H), 4.98–4.63 (m, 4H), 3.90 (t, *J* = 4.8 Hz, 4H), 3.75 (t, *J* = 4.7 Hz, 4H), 3.49 (s, 3H), 3.28–3.26 (m, 4H). LC/MS (ESI+): *m/z* 386.1 (M + H).

**5-(6-(3-(2-Methoxyethoxy)oxetan-3-yl)-4-morpholinothieno[3,2-*d*]pyrimidin-2-yl)pyrimidin-2-amine (11).** To a slurry of **26** (0.15 g, 0.38 mmol) and 2-aminopyrimidine-5-boronic acid, pinacol ester (0.13 g, 0.56 mmol) in 1 M aqueous KOAc (0.75 mL) and acetonitrile (0.97 mL) was degassed by bubbling nitrogen through the solution for 10 min. Next, bis(ditert-butyl(4-

dimethylaminophenyl)phosphine)dichloropalladium(II) (0.03 g, 0.04 mmol) was added to the solution under a tent of nitrogen. The reaction mixture was heated in a Biotage microwave at 130 °C for 30 min. The reaction mixture was diluted with a large volume of EtOAc and an equal portion of 2 N HCl. This mixture was vacuum filtered to remove a black precipitate. The organic and aqueous layers were separated, and the acidic aqueous layer was lyophilized to dryness. The resulting dry powder was combined with the organic layer and concentrated and purified by HPLC to provide **11** (50 mg, 30% yield). <sup>1</sup>H NMR (400 MHz, DMSO) δ 9.12 (s, 2H), 7.69 (s, 1H), 7.07 (s, 2H), 4.85 (s, 4H), 3.96 (t, *J* = 4.6 Hz, 4H), 3.78 (t, *J* = 4.8 Hz, 4H), 3.49 (s, 4H), δ 3.29 (s, 3H). LC/MS (ESI+): *m/z* 445.2 (M + H).

**5-(6-(1,1-Difluoroethyl)-4-morpholinothieno[3,2-*d*]pyrimidin-2-yl)pyrimidin-2-amine (12).** 1-(2-Chloro-4-morpholinothieno[3,2-*d*]pyrimidin-6-yl)ethanol<sup>5</sup> (400 mg, 1.0 mmol) was dissolved in methylene chloride (8.6 mL, 130 mmol). Manganese(IV)oxide (0.58 g, 7.7 mmol) was added and the reaction stirred overnight. The reaction mixture was filtered and concentrated under reduced pressure. The residue was dissolved in methylene chloride (20 mL, 300 mmol). Bis(2-methoxyethyl)aminosulfur trifluoride (0.995 mL, 4.63 mmol) was added, followed by ethanol (13.5 uL, 0.232 mmol). The reaction stirred 72 h, bis(2-methoxyethyl)aminosulfur trifluoride (1.99 mL, 9.27 mmol) was added, and reaction was stirred overnight. The reaction was quenched with saturated aqueous NaHCO<sub>3</sub> and extracted with methylene chloride, washed with brine, dried over MgSO<sub>4</sub>, filtered, and concentrated under reduced pressure. The residue was partially purified by silica gel chromatography (0–100% EtOAc in heptanes) to give 4-(2-chloro-6-(1,1-difluoroethyl)thieno[3,2-*d*]pyrimidin-4-yl)-morpholine (300 mg, LCMS (ESI): *m/z* = 320.1 [M + H]<sup>+</sup>). A portion of the intermediate (111 mg, 0.35 mmol) was combined with 5-(4,4,5,5-tetramethyl-1,3,2-dioxaborolan-2-yl)pyrimidin-2-amine (0.23 g, 1.0 mmol), tetrakis(triphenylphosphine)palladium(0) (0.02 g, 0.02 mmol), 1.0 M potassium acetate in water (0.69 mL), and acetonitrile (2.0 mL) in a microwave vial. The vessel was sealed and heated at 140 °C for 20 min in a Biotage Initiator microwave. Upon cooling, the aqueous layer was removed, and the organic layer was concentrated under reduced pressure. The residue was purified by HPLC to give **12** (42 mg, 13% yield over 2 steps). <sup>1</sup>H NMR (400 MHz, DMSO-*d*<sub>6</sub>) δ 9.12 (s, 2H), 7.86 (s, 1H), 7.12 (s, 2H), 3.99 (t, *J* = 4.7 Hz, 4H), 3.79 (t, *J* = 4.8 Hz, 4H), 2.20 (t, *J* = 18.8 Hz, 3H). LCMS (ESI): *m/z* = 379.2 [M + H]<sup>+</sup>.

**4-(6-(Azetidin-3-yl)-2-chlorothieno[3,2-*d*]pyrimidin-4-yl)-morpholine.** Compound **19** (1.5 g, 3.6 mmol) was treated with TFA (2 mL) in CH<sub>2</sub>Cl<sub>2</sub> (2 mL), and stirred at room temperature 1 h. Saturated aqueous NaHCO<sub>3</sub> was added, and the aqueous layer was extracted with 10% MeOH/EtOAc, dried over MgSO<sub>4</sub>, filtered, and concentrated to give 4-(6-(azetidin-3-yl)-2-chlorothieno[3,2-*d*]pyrimidin-4-yl)morpholine (1.1 g, 70% yield). LC/MS (ESI+): *m/z* 311.2 (M + H).

**1-(3-(2-Chloro-4-morpholinothieno[3,2-*d*]pyrimidin-6-yl)-azetidin-1-yl)ethanone.** To a mixture of 4-(6-(azetidin-3-yl)-2-chlorothieno[3,2-*d*]pyrimidin-4-yl)morpholine (80 mg, 0.2 mmol) in CH<sub>2</sub>Cl<sub>2</sub> (0.33 mL) was added triethylamine (0.11 mL, 0.77 mmol) followed by acetic anhydride (0.027 mL, 0.28 mmol). The reaction mixture stirred for 1 h at room temperature. The reaction was concentrated under reduced pressure and purified by silica gel chromatography (5% MeOH/EtOAc) to give 1-(3-(2-chloro-4-morpholinothieno[3,2-*d*]pyrimidin-6-yl)azetidin-1-yl)ethanone (60 mg, 70% yield). <sup>1</sup>H NMR (400 MHz, CDCl<sub>3</sub>) δ 7.23–7.09 (d, *J* = 2.3 Hz, 1H), 4.68–4.55 (t, *J* = 8.2 Hz, 1H), 4.55–4.41 (t, *J* = 11.3 Hz, 1H), 4.28–4.19 (m, 1H), 4.18–4.05 (m, 2H), 4.05–3.91 (m, 4H), 3.88–3.76 (t, *J* = 4.6 Hz, 4H), 2.03–1.83 (d, *J* = 2.2 Hz, 3H). LC/MS (ESI+): *m/z* 353.3 (M + H).

**1-(3-(2-(2-Aminopyrimidin-5-yl)-4-morpholinothieno[3,2-*d*]pyrimidin-6-yl)azetidin-1-yl)ethanone (13).** To a microwave vial was added 1-(3-(2-chloro-4-morpholinothieno[3,2-*d*]pyrimidin-6-yl)-azetidin-1-yl)ethanone (90 mg, 0.2 mmol), 2-aminopyrimidine-5-boronic acid, pinacol ester (82 mg, 0.37 mmol), and 1 M cesium carbonate solution in water (0.74 mL, 0.7 mmol) followed by 1,1'-



bis(diphenylphosphino)ferrocenepalladium(II) chloride (20 mg, 0.02 mmol). The mixture was degassed under nitrogen for 5 min and then subjected to microwave irradiation at 140 °C for 20 min. The crude mixture was filtered through a thin layer of Celite, and the filtered organics were diluted with EtOAc and washed with water. The organic layer was concentrated under reduced pressure and purified by HPLC to give **13** (49 mg, 48% yield). <sup>1</sup>H NMR (400 MHz, DMSO) δ 9.19–8.99 (s, 2H), 7.55–7.38 (s, 1H), 7.22–6.93 (s, 2H), 4.71–4.49 (t, *J* = 8.0 Hz, 1H), 4.41–4.14 (m, 3H), 4.06–3.87 (m, 5H), 3.87–3.70 (t, *J* = 4.7 Hz, 4H), 1.88–1.66 (s, 3H). LC/MS (ESI+): *m/z* 412.2 (M + H).

**5-(7-Methyl-6-(3-(methylsulfonyl)phenyl)-4-morpholinethieno[3,2-*d*]pyrimidin-2-yl)pyrimidin-2-amine (14).** 4-(2-Chloro-6-iodo-7-methylthieno[3,2-*d*]pyrimidin-4-yl)morpholine<sup>21</sup> (0.6 g, 1.5 mmol), 4,4,5,5-tetramethyl-2-(3-(methylsulfonyl)phenyl)-1,3,2-dioxaborolane (0.3 g, 1.5 mmol), 1 M Na<sub>2</sub>CO<sub>3</sub> (5 mL), acetonitrile (5 mL), and PdCl<sub>2</sub>(PPh<sub>3</sub>)<sub>2</sub> were combined in a microwave vial. The vessel was sealed and heated to 100 °C for 15 min in a Biotage Initiator microwave. Upon cooling, the aqueous layer was removed and the organic layer was concentrated under reduced pressure. The residue was partially purified by silica gel chromatography (0–40% EtOAc in methylene chloride) to give 157 mg of 4-(2-chloro-7-methyl-6-(3-(methylsulfonyl)phenyl)thieno[3,2-*d*]pyrimidin-4-yl)morpholine. To partially purified 4-(2-chloro-7-methyl-6-(3-(methylsulfonyl)phenyl)thieno[3,2-*d*]pyrimidin-4-yl)morpholine (0.47 g, 1.1 mmol) were added 5-(4,4,5,5-tetramethyl-1,3,2-dioxaborolan-2-yl)pyrimidin-2-amine (0.365 g, 1.65 mmol), tetrakis(triphenylphosphine)palladium(0) (0.064 g, 0.055 mmol), 1.0 M potassium acetate in water (4.5 mL), and acetonitrile (4.5 mL) in a microwave vial. The vessel was sealed and heated to 150 °C for 20 min in a Biotage Initiator microwave. Upon cooling, the reaction mixture was filtered and concentrated under reduced pressure. The residue was rinsed with water and EtOAc, and the combined liquids were lyophilized. The resulting product was dissolved in 100 mL of methanol, and 4 equiv of 4 N HCl in dioxane were added. The mixture was stirred 5 h at room temperature and then was concentrated under reduced pressure. The solid was taken up in water (100 mL) and filtered, followed by lyophilization for 3 days to give **14** as the HCl salt of (0.10 g, 5% over two steps). <sup>1</sup>H NMR (400 MHz, DMSO-*d*<sub>6</sub>) δ 9.36(s, 2H), 8.18 (s, 1H), 8.01 (s, 1H), 7.90 (s, 2H), 7.80 (s, 2H), 4.06 (t, *J* = 4.7 Hz, 4H), 3.90 (t, *J* = 4.8 Hz, 4H), 3.13 (s, 3H), 2.57 (s, 3H). LCMS (ESI): *m/z* = 483.1 [M = H]<sup>+</sup>.

**4-(7-Bromo-2-chlorothieno[3,2-*d*]pyrimidin-4-yl)morpholine (28).** 7-Bromo-2,4-dichlorothieno[3,2-*d*]pyrimidine (27)<sup>19</sup> (2.9 g, 10.0 mmol) was dissolved in methanol (100 mL) and added morpholine (2 mL, 22 mmol), and the reaction mixture was stirred for 1.5 h. The reaction mixture was concentrated, diluted with water, extracted with CH<sub>2</sub>Cl<sub>2</sub>, and concentrated. The product was purified by silica gel chromatography (0–100% EtOAc/heptanes) to give **28** (1.2 g, 35% yield). <sup>1</sup>H NMR (400 MHz, CDCl<sub>3</sub>) δ 7.78 (s, 1H), 4.01 (m, 4H), 3.85 (m, 4H). LCMS (ESI): *m/z* = 336.0 [M = H]<sup>+</sup>.

**4-(2-Chloro-7-vinylthieno[3,2-*d*]pyrimidin-4-yl)morpholine (29).** Compound **28** (3.55 g, 10.6 mmol), (2-ethenyl)tri-*n*-butyltin (3.41 mL, 11.7 mmol), Pd(PPh<sub>3</sub>)<sub>4</sub> (613 mg, 0.53 mmol), and 1,4-dioxane (30 mL, 400 mmol) were combined in a sealed tube and heated 19.5 h at 100 °C. The reaction mixture was concentrated and purified by silica gel chromatography (0–50% EtOAc/heptanes) to give **29** (1.18 g, 40% yield). <sup>1</sup>H NMR (400 MHz, CDCl<sub>3</sub>) δ 7.72(s, 1H), 7.04 (q, *J* = 17.7, 11.2 Hz, 1H), 6.10 (d, *J* = 17.9, 1.3 Hz, 1H), 5.44 (d, *J* = 11.2, 1.3 Hz, 1H), 4.01 (t, *J* = 5.7, 4.0 Hz, 4H), 3.85 (t, 4 H). LCMS (ESI): *m/z* = 338.1 [M = H]<sup>+</sup>.

**2-(2-Chloro-7-(2-hydroxyethyl)-4-morpholinethieno[3,2-*d*]pyrimidin-6-yl)propan-2-ol (30).** Compound **29** (170 mg, 0.6 mmol) was dissolved in tetrahydrofuran (10 mL, 100 mmol) and cooled to 0 °C under an atmosphere of nitrogen. Then 0.5 M 9-BBN in hexanes (3.4 mL, 2 mmol) was added, and the reaction was warmed to room temperature and stirred overnight. LCMS indicated mostly starting material, so the reaction was cooled to 0 °C again and 0.5 M 9-BBN in hexanes (8.0 mL, 4 mmol) was added, and the reaction mixture was warmed to room temperature and stirred overnight.

Hydrogen peroxide (20 M, 1.4 mL, 20 mmol) was added followed by 5 M sodium hydroxide in water (2.4 mL, 10 mmol). The reaction was diluted with water, extracted with EtOAc, dried over MgSO<sub>4</sub>, and concentrated. The crude mixture was partially purified by silica gel chromatography (0–50% EtOAc/heptanes) to give 2-(2-chloro-4-morpholinethieno[3,2-*d*]pyrimidin-7-yl)ethanol (110 mg). A portion of the partially purified intermediate (70 mg, 0.2 mmol) was dissolved in THF (5 mL, 60 mmol) and cooled to –40 °C. *n*-BuLi in hexanes (2.5 M, 370 mL, 0.93 mmol) was added and stirred for 1 h. Acetone (86 μL, 1.2 mmol) was added and then stirred at –40 °C for 5 h. Reaction was quenched with saturated NH<sub>4</sub>Cl and extracted with EtOAc, dried over MgSO<sub>4</sub>, and concentrated to give **30** (30 mg, 36% yield over 2 steps).

**5-(8,8-Dimethyl-1-morpholin-4-yl)-5,8-dihydro-6H-7-oxa-9-thia-2,4-diazafloren-3-yl)-pyrimidin-2-ylamine (15).** Intermediate **30** (30 mg) was dissolved in toluene (5 mL, 50 mmol). Trifluoroacetic acid (0.5 mL, 6 mmol) was added, and the reaction mixture was heated 2 h at 120 °C. The reaction mixture was diluted with water and extracted with EtOAc, dried over MgSO<sub>4</sub>, concentrated, and partially purified by silica gel chromatography (0–100% EtOAc/heptanes) to give 3-chloro-8,8-dimethyl-1-morpholin-4-yl-5,8-dihydro-6H-7-oxa-9-thia-2,4-diazafloren-3-yl)-pyrimidin-2-ylamine (10 mg). The intermediate chloropyrimidine (10 mg, 0.03 mmol) was dissolved in acetonitrile (2 mL, 40 mmol), and 1 M sodium carbonate in water (2 mL, 2 mmol), 5-(4,4,5,5-tetramethyl-1,3-dioxolan-2-yl)pyrimidin-2-amine (9.0 mg, 0.041 mmol), and bis(ditert-butyl(4-dimethylaminophenyl)phosphine)dichloropalladium (1.1 mg) were added. The reaction was irradiated by microwave at 120 °C for 15 min. The aqueous layer was removed, and the organic layer was concentrated and purified by silica gel chromatography (0–100% EtOAc/heptanes) to give **15** (3 mg, 2% yield over 2 steps). <sup>1</sup>H NMR (400 MHz, CDCl<sub>3</sub>) δ 9.30 (s, 2H), 5.34 (br s, 2H), 4.08 (t, 2H), 4.01 (m, 4H), 3.87 (m, 4H), 2.95 (t, 2H), 1.62 (s, 6H). LCMS (ESI): *m/z* = 399.3 [M = H]<sup>+</sup>.

**4-(2-Chloro-6-(3,3-dimethyloxetan-2-yl)thieno[3,2-*d*]pyrimidin-4-yl)morpholine.** Compound **17**<sup>6</sup> (0.6 g, 2.3 mmol) was suspended in THF (10 mL) and cooled to –78 °C, 2.5 M *n*-BuLi (1.2 equiv) was added dropwise and the reaction was warmed to –40 °C and stirred 1 h. After 1 h, the reaction was cooled to –78 °C and treated with 2,2-dimethyl-3-oxopropyl 4-methylbenzenesulfonate<sup>22</sup> (0.4 g, 2.0 mmol). The reaction was warmed to room temperature and stirred for 1 h. The reaction was poured into saturated aqueous NH<sub>4</sub>Cl and extracted with EtOAc. The organic extracts were washed with water and brine, dried over MgSO<sub>4</sub>, filtered, and concentrated. The crude reaction was purified by silica gel chromatography (0–70% EtOAc/hexane) to give 4-(2-chloro-6-(3,3-dimethyloxetan-2-yl)thieno[3,2-*d*]pyrimidin-4-yl)morpholine (0.3 g, 60% yield). <sup>1</sup>H NMR (400 MHz, DMSO) δ 7.32–7.12 (s, 1H), 5.86–5.72 (s, 1H), 4.53–4.39 (d, *J* = 5.6 Hz, 1H), 4.36–4.25 (d, *J* = 5.6 Hz, 1H), 4.02–3.83 (t, *J* = 4.8 Hz, 4H), 3.83–3.66 (t, *J* = 4.5 Hz, 4H), 1.48–1.31 (s, 3H), 1.02–0.86 (s, 3H). LC/MS (ESI+): *m/z* 340.2 (M + H).

**5-(6-(3,3-Dimethyloxetan-2-yl)-4-morpholinethieno[3,2-*d*]pyrimidin-2-yl)pyrimidin-2-amine (16).** To a microwave vial was added 4-(2-chloro-6-(3,3-dimethyloxetan-2-yl)thieno[3,2-*d*]pyrimidin-4-yl)morpholine (300 mg, 1.0 mmol), 2-aminopyrimidine-5-boronic acid, pinacol ester (290 mg, 1.3 mmol), and 1 M cesium carbonate solution in water (1.8 mL, 1.8 mmol) followed by 1,1'-bis(diphenylphosphino)ferrocenepalladium(II) chloride (65 mg, 0.08 mmol). The mixture was degassed under nitrogen for 5 min and then subjected to microwave at 140 °C for 30 min. The crude mixture was filtered through a thin layer of Celite, and the filtered organics were diluted with EtOAc and washed with water. The organic layer was concentrated under reduced pressure and purified by SFC to give **16** (37 mg, 11% yield). <sup>1</sup>H NMR (400 MHz, DMSO) δ 9.24–8.98 (s, 2H), 7.40–7.20 (d, *J* = 1.2 Hz, 1H), 7.15–7.01 (s, 2H), 5.97–5.66 (s, 1H), 4.53–4.39 (d, *J* = 5.6 Hz, 1H), 4.38–4.24 (d, *J* = 5.6 Hz, 1H), 4.07–3.90 (dd, *J* = 6.0, 3.5 Hz, 4H), 3.88–3.71 (t, *J* = 4.7 Hz, 4H), 1.53–1.29 (s, 3H), 1.04–0.87 (s, 3H). LC/MS (ESI+): *m/z* 399.2 (M + H).

**Characterization of Biochemical and Cellular Activity in Vitro.** Enzymatic activity of the PI3K $\alpha$  was measured using a fluorescence polarization assay that monitors formation of the product 3,4,5-inositoltriphosphate molecule (PIP3) as it competed with fluorescently labeled PIP3 for binding to the GRP-1 pleckstrin homology domain protein. An increase in phosphatidyl inositide-3-phosphate product resulted in a decrease in fluorescence polarization signal as the labeled fluorophore was displaced from the GRP-1 protein binding site. PI3K $\alpha$  was purchased from Perkin-Elmer or was expressed and purified as a heterodimeric recombinant protein. Tetramethylrhodamine-labeled PIP3 (TAMRA-PIP3), di-C8-PIP2, and PIP3 detection reagents were purchased from Echelon Biosciences. PI3K $\alpha$  was assayed under initial rate conditions in the presence of 10 mM Tris (pH 7.5), 25  $\mu$ M ATP, 9.75  $\mu$ M PIP2, 5% glycerol, 4 mM MgCl<sub>2</sub>, 50 mM NaCl, 0.05% (v/v) Chaps, 1 mM dithiothreitol, and 2% (v/v) DMSO at a 60 ng/mL concentration of PI3K $\alpha$ . After assay for 30 min at 25 °C, reactions were terminated with a final concentration of 9 mM EDTA, 4.5 nM TAMRA-PIP3, and 4.2  $\mu$ g/mL GRP-1 detector protein before reading fluorescence polarization on an Envision plate reader. IC<sub>50</sub>'s were calculated from the fit of the dose–response curves to a four-parameter equation. Apparent K<sub>i</sub> values, where measured, were determined at a fixed concentration of ATP near the measured K<sub>m</sub> for ATP for PI3K $\alpha$  and were calculated by fitting of the dose–response curves to an equation for tight-binding competitive inhibition. All IC<sub>50</sub>'s and apparent K<sub>i</sub> values represent geometric means of at least three determinations. These assays generally produced results within 2-fold of the reported mean.

Human recombinant mTOR(1360–2549) was expressed and purified from insect cells and assayed using a Lanthascreen fluorescence resonance energy transfer format from Invitrogen in which phosphorylation of recombinant green fluorescent protein (GFP)-4-EBP1 was detected using a terbium-labeled antibody to phospho-threonine 37/46 of 4-EBP1. Reactions were initiated with ATP and conducted in the presence of 50 mM Hepes (pH 7.5), 0.25 nM mTOR, 400 nM GFP-4E-BP1, 8  $\mu$ M ATP, 0.01% (v/v) Tween 20, 10 mM MnCl<sub>2</sub>, 1 mM EGTA, 1 mM dithiothreitol, and 1% (v/v) DMSO. Assays were conducted under initial rate conditions at room temperature for 30 min before terminating the reaction and detecting product in the presence of 2 nM Tb-anti-p4E-BP1 antibody and 10 mM EDTA. Dose–response curves were fit to an equation for competitive tight-binding inhibition and apparent K<sub>s</sub> were calculated using the determined K<sub>m</sub> for ATP of 6.1  $\mu$ M. All apparent K<sub>i</sub> values represent geometric means of minimum of two determinations. These assays generally produced results within 2-fold of the reported mean.

Antiproliferative cellular assays were conducted using PC3 human tumor cell lines provided by the ATCC. Cell lines were cultured in RPMI supplemented with 10% fetal bovine serum, 100 units/mL penicillin, and 100  $\mu$ g/mL streptomycin, 10 mM HEPES, and 2 mM glutamine at 37 °C under 5% CO<sub>2</sub>. PC3 cells were seeded in 384-well plates in media at 1000 or 3000 cells/well, respectively, and incubated overnight prior to the addition of compounds to a final DMSO concentration of 0.5% v/v. PC3 cells were incubated for 3 and 4 days, respectively, prior to the addition of CellTiter-Glo reagent (Promega) and reading of luminescence using an Analyst plate reader. For antiproliferative assays, a cytostatic agent such as aphidicolin and a cytotoxic agent such as staurosporine were included as controls. Dose–response curves were fit to a four-parameter equation and relative EC<sub>50</sub>'s were calculated using Assay Explorer or Genedata software. All cellular EC<sub>50</sub> values represent geometric means of a minimum of at least two determinations and these assays generally produced results within 3-fold of the reported mean.

**Glioma Cell Activity.** Cell lines were cultured in RPMI supplemented with 10% fetal bovine serum, 100 units/mL penicillin, and 100  $\mu$ g/mL streptomycin at 37 °C under 5% CO<sub>2</sub>. Cells were seeded (1000–2000 cells/well) in 384-well plates for 16 h. On day two, nine serial 1:2 compound dilutions were made in DMSO in a 96-well plate. The compounds were then further diluted into growth media using a Rapidplate robot (Zymark Corp., Hopkinton, MA). The diluted compounds were then added to quadruplicate wells in the 384-well cell plate and incubated at 37 °C and 5% CO<sub>2</sub>. After 4 days, relative

numbers of viable cells were measured by luminescence using CellTiter Glo (Promega) according to the manufacturer's instructions and read on a Wallac Multilabel Reader (PerkinElmer, Foster City). EC<sub>50</sub>'s were calculated using Prism 4.0 software (Graph pad, San Diego). Typical variability of EC<sub>50</sub>'s of a control compound in these assays was less than 2-fold.

**In Vitro Transport Assays.** Madin–Darby canine kidney (MDCK) cells heterologously expressing human P-gp, human BCRP, or mouse Bcrp1, and LLC-PK1 cells transfected with mouse P-gp (mdr1a) were used to determine whether compounds are substrate of these transporters. MDR1-MDCKI cells were licensed from the NCI (National Cancer Institute, Bethesda, MD), while Bcrp1-MDCKII, BCRP-MDCKII, and Mdr1a-LLC-PK1 cells were obtained from The Netherlands Cancer Institute (Amsterdam, The Netherlands). For transport studies, cells were seeded on 24-well Millicell plates (Millipore, Billerica, MA) 4 days prior to use (polyethylene terephthalate membrane, 1  $\mu$ m pore size) at a seeding density of 2.5  $\times$  10<sup>5</sup> cells/mL (except for MDR1-MDCKI, 1.3  $\times$  10<sup>5</sup> cells/mL). Compounds were tested at 5  $\mu$ M in the apical to basolateral (A–B) and basolateral to apical (B–A) directions. The compounds were dissolved in transport buffer consisting of Hank's Balanced Salt Solution (HBSS) with 10 mM HEPES (Invitrogen Corporation, Grand Island, NY). Lucifer Yellow (Sigma-Aldrich, St. Louis, MO) was used as the paracellular marker. Compound concentrations in the donor and receiving compartments were determined by LC-MS/MS analysis. The apparent permeability (P<sub>app</sub>), in the apical to A–B and B–A directions, was calculated after a 2 h incubation as:

$$P_{app} = (dQ/dt) \cdot (1/AC_0)$$

Where dQ/dt = rate of compound appearance in the receiver compartment, A = surface area of the insert, and C<sub>0</sub> = initial substrate concentration at T<sub>0</sub>.

The efflux ratio (ER) was calculated as (P<sub>app, B–A</sub>/P<sub>app, A–B</sub>).

All efflux ratios reported represent the arithmetic mean of a minimum of at least two determinations, and these assays generally produced results within 50% of the reported mean.

**Determination of Plasma Protein and Brain Binding.** The extent of protein binding was determined in vitro in mouse plasma (Bioreclamation, Inc., Hicksville, NY) by equilibrium dialysis using a HTDialysis 96-well block (HTDialysis LLC; Gales Ferry, CT). The compound was added to pooled plasma from multiple animals (n  $\geq$  3) at a total concentration of 10  $\mu$ M. Plasma samples were equilibrated with phosphate-buffered saline (pH 7.4) at 37 °C in 90% humidity and 5% CO<sub>2</sub> for 4 h. Following dialysis, concentration of compounds in plasma and buffer were measured by LC-MS/MS. The percent unbound in plasma was determined by dividing the concentration measured in the postdialysis buffer by that measured in the postdialysis plasma and multiplying by 100. Incubations were performed in triplicate, and coefficient of variation was not greater than 30%.

The free fraction in mouse brain was determined as described by Kalvass.<sup>23</sup> Briefly, brain tissue was homogenized in 3 volumes of phosphate-buffered saline and compound was added at a final concentration of 10  $\mu$ M. Aliquots of 300  $\mu$ L were dialyzed in a RED device (Thermo Scientific, Rockford, IL) against a volume of 500  $\mu$ L of buffer for 4 h at 37 °C in an incubator at 90% humidity and 5% CO<sub>2</sub>. Following dialysis, tissues and buffer samples were analyzed as described for the plasma protein binding studies.

**Pharmacokinetic Studies in Mice.** Twelve female CD-1 mice (Charles River Laboratories, Hollister, CA) were given an oral (PO) dose of the indicated compound in 0.5% methylcellulose/0.2% Tween 80 (MCT). Two blood samples of approximately 0.15 mL were collected from each mouse (n = 3 mice per time point) by retro-orbital bleed or terminal cardiac puncture while the animals were anesthetized with isoflurane. Blood samples were collected in tubes containing K2EDTA as the anticoagulant, predose and at 0.083, 0.25, 0.5, 1, 3, 6, 9, and 24 h postdose. Samples were centrifuged within 1 h of collection and plasma was collected and stored at –80 °C until analysis. Total concentrations of the compound were determined by liquid chromatography–tandem mass spectrometry (LC-MS/MS),



following plasma protein precipitation with acetonitrile and injection of the supernatant onto the column, a Varian MetaSil AQ-C18 column (50 mm × 2 mm, 5 μm particle size). A CTC HTS PAL autosampler (LEAP Technologies, Chapel Hill, NC) linked to a Shimadzu SCL-10A controller with LC-10AD pumps (Shimadzu, Columbia MD), coupled with an AB Sciex API 4000 triple quadrupole mass spectrometer (AB Sciex, Foster City, CA) were used for the LC-MS/MS assay. The aqueous mobile phase was water with 0.1% formic acid, and the organic mobile phase was acetonitrile with 0.1% formic acid. The lower and upper limits of quantitation of the assay were 0.005 and 10 μM, respectively. The total run time was 1.5 min, and the ionization was conducted in the positive ion mode. Where brain concentration was determined, brains were collected at 1 and 6 h postdose from three different animals at each time point, rinsed with ice-cold saline, weighed, and stored at -80 °C until analysis. For compound quantitation, mouse brains were homogenized in 3 volumes of water. The homogenates were extracted by protein precipitation with acetonitrile. LC-MS/MS analysis was conducted as described for the plasma. Brain homogenate concentrations were converted to brain concentrations for the calculations of brain-to-plasma ratios.

**Modulation of pAKT in Brain.** Female CD-1 mice were administered a single PO dose of the indicated compound. Brains and plasma were collected at the indicated time postdose from three animals at each time point. Individual brains were split in half for PD analysis and compound concentration measurement. The samples were stored at -70 °C and analyzed for total concentration. For PD analysis, cell extraction buffer (Invitrogen, Camarillo, CA) containing 10 mM Tris pH 7.4, 100 mM NaCl, 1 mM EDTA, 1 mM EGTA, 1 mM NaF, 20 mM Na<sub>4</sub>P<sub>2</sub>O<sub>7</sub>, 2 mM Na<sub>3</sub>VO<sub>4</sub>, 1% Triton X-100, 10% glycerol, 0.1% SDS, and 0.5% deoxycholate was supplemented with phosphatase, protease inhibitors (Sigma, St. Louis, MO), and 1 mM PMSF and added to frozen brain biopsies. Brains were homogenized with a small pestle (Konte Glass Company, Vineland, NJ), sonicated briefly on ice, and centrifuged at 20000g for 20 min at 4 °C. Protein concentration was determined using BCA protein assay (Pierce, Rockford, IL). Proteins were separated by electrophoresis and transferred to NuPage nitrocellulose membranes (Invitrogen, Camarillo, CA). Licor Odyssey infrared detection system (Licor, Lincoln, NE) was used to assess and quantify protein expression. PI3K pathway markers were evaluated by immunoblotting using antibodies against pAkt<sup>ser473</sup> and total Akt (Invitrogen, Camarillo, CA and Cell Signaling, Danvers, MA). Inhibition of pAkt (%) was calculated by comparing pAkt signal with that measured in untreated mice.

**In Vivo Xenograft Studies.** All in vivo studies were conducted in compliance with Genentech's Institutional Animal Care and Use Committee. PTEN-null U-87 MG/M human glioblastoma cancer cells (an in-house derivative of U-87 MG cells from American Type Culture Collection (Manassas, VA)) were cultured in RPMI 1640 media plus 1% L-glutamine with 10% fetal bovine serum (HyClone; Waltham, MA). Cells in log-phase growth were harvested and resuspended in HBSS:Matrigel (BD Biosciences (Franklin Lakes, NJ)) (1:1, v:v) for injection into female NCr nude mice (Taconic Farms (Cambridge City, IN)) aged 10 weeks. Animals received five million cells subcutaneously in the right lateral thorax in 0.1 mL. Mice bearing established tumors in the range of 180–350 mm<sup>3</sup> were separated into groups of equally sized tumors ( $n = 5-7/\text{group}$ ) to receive escalating doses of 7 and 9. Both inhibitors were formulated once weekly in 0.5% methylcellulose and 0.2% Tween-80 at concentrations needed for target doses in a volume of 0.2 mL. Tumor volumes were calculated from perpendicular length and width caliper measurements using the formula: tumor volume (mm<sup>3</sup>) = 0.5(length × width<sup>2</sup>). Changes in body weights are reported as a percentage change from the starting weight.

A mixed modeling approach was used to analyze the repeated measurement of tumor volumes from the same animals over time since this approach addresses both repeated measurements as well as modest dropouts before study end (Pinheiro et al. 2008). Log<sub>2</sub> (tumor volume) growth traces were fitted to each dose group with restricted cubic splines for the dose and fixed time effects for each inhibitor.

Fitting was done via a linear mixed-effects model, using the R package nlme (version 3.1–97) in R version 2.13.0 (R Development Core Team 2008; R Foundation for Statistical Computing (Vienna, Austria)). Fitted tumor volumes were plotted in the natural scale in Prism (version 5.0b for Mac) (GraphPad Software (La Jolla, CA)).

## ■ ASSOCIATED CONTENT

### 📄 Supporting Information

Tumor growth inhibition plots including additional doses studied and body weight plots. This material is available free of charge via the Internet at <http://pubs.acs.org>.

## ■ AUTHOR INFORMATION

### Corresponding Author

\*Phone: (650) 467-3214. Fax: (650) 225-2061. E-mail: [thefron@gene.com](mailto:thefron@gene.com).

### Notes

The authors declare no competing financial interest.

## ■ ACKNOWLEDGMENTS

We thank Mengling Wong, Chris Hamman, Michael Hayes, Steve Huhn, and Wen Chiu for compound purification and determination of purity by HPLC, mass spectroscopy and <sup>1</sup>H NMR. We thank Krista K. Bowman, Alberto Estevez, Kyle Mortara, and Jiansheng Wu for technical assistance of protein expression and purification.

## ■ ABBREVIATIONS USED

PI3K, phosphoinositide 3-kinase; GBM, glioblastoma multiforme; BBB, blood–brain barrier; PTEN, phosphatase and tensin homologue; mTOR, mammalian target of rapamycin; P-gp, P-glycoprotein; Bcrp1, breast cancer resistance protein; MDCK, Madin–Darby canine kidney; MDR1, multidrug resistance gene; CNS, central nervous system; TPSA, topological polar surface area; MW, molecular weight; HBD, hydrogen bond donors; CNS MPO, central nervous system multiparameter optimization; Cl<sub>w</sub>, unbound clearance; PPB, plasma protein binding; AKT, protein kinase B; S6RP, ribosomal protein S6; DMA, N,N-dimethylacetamide; TFA, trifluoroacetic acid; THF, tetrahydrofuran; DMF, dimethylformamide

## ■ REFERENCES

- (1) Liu, P.; Cheng, H.; Roberts, T. M.; Zhou, J. J. Targeting the Phosphoinositide 3-Kinase Pathway in Cancer. *Nature Rev. Drug Discovery* **2009**, *8*, 627.
- (2) Akhavan, D.; Cloughesy, T. F.; Mischel, P. S. mTOR Signaling in Glioblastoma: Lessons Learned From Bench to Bedside. *Neuro-Oncology (Durham, NC, U. S.)* **2010**, *12*, 882–889.
- (3) The Cancer Genome Atlas Network. Comprehensive genomic characterization defines human glioblastoma genes and core pathways. *Nature* **2008**, *455*, 1061–1068.
- (4) Folkes, A. J.; Ahmadi, K.; Alderton, W. K.; Alix, S.; Baker, S. J.; Box, G.; Chuckowree, I. S.; Clarke, P. A.; Depledge, P.; Eccles, S. A.; Friedman, L. S.; Hayes, A.; Hancox, T. C.; Kugendradas, A.; Lensun, L.; Moore, P.; Olivero, A. G.; Pang, J.; Patel, S.; Pergl-Wilson, G. H.; Raynaud, F. I.; Robson, A.; Saghir, N.; Salphati, L.; Sohal, S.; Ultsch, M. H.; Valenti, M.; Wallweber, H. J. A.; Wan, N. C.; Wiesmann, C.; Workman, P.; Zhyvoloup, P.; Zvelebil, M. J.; Shuttleworth, S. J. The Identification of 2-(1H-Indazol-4-yl)-6-(4-methanesulfonyl-piperazin-1-ylmethyl)-4-morpholin-4-yl-thieno[3,2-d]pyrimidine (GDC-0941) as a Potent, Selective, Orally Bioavailable Inhibitor of Class I PI3 Kinase for the Treatment of Cancer. *J. Med. Chem.* **2008**, *51*, 5522–5532.



- (5) Sutherlin, D. P.; Sampath, D.; Berry, M.; Castanedo, G.; Chang, Z.; Chuckowree, I.; Dotson, J.; Folkes, A.; Friedman, L.; Goldsmith, R.; Heffron, T.; Lee, L.; Lesnick, J.; Lewis, C.; Mathieu, S.; Nonomiya, J.; Olivero, A.; Pang, J.; Prior, W. W.; Salphati, L.; Sideris, S.; Tian, Q.; Tsui, V.; Wan, N. C.; Wang, S.; Wiesmann, C.; Wong, S.; Zhu, B.-Y. Discovery of (Thienopyrimidin-2-yl)aminopyrimidines as Potent, Selective, and Orally Available Pan-PI3-Kinase and Dual Pan-PI3-Kinase/mTOR Inhibitors for the Treatment of Cancer. *J. Med. Chem.* **2010**, *53*, 1086–1097.
- (6) Sutherlin, D. P.; Bao, L.; Berry, M.; Castanedo, G.; Chuckowree, I.; Dotson, J.; Folkes, A.; Friedman, L.; Goldsmith, R.; Gunzner, J.; Heffron, T.; Lesnick, J.; Lewis, C.; Mathieu, S.; Murray, J.; Nonomiya, J.; Pang, J.; Pegg, N.; Prior, W. W.; Rouge, L.; Salphati, L.; Sampath, D.; Tian, Q.; Tsui, V.; Wan, N. C.; Wang, S.; Wei, B. Q.; Weismann, C.; Wu, P.; Zhu, B.-Y.; Olivero, A. Discovery of a Potent, Selective, and Orally Available Class I Phosphatidylinositol 3-Kinase (PI3K)/Mammalian Target of Rapamycin (mTOR) Kinase Inhibitor (GDC-0980) for the Treatment of Cancer. *J. Med. Chem.* **2011**, *54*, 7579–7587.
- (7) Where MDR1 and Bcrp1 efflux ratios are reported within this article,  $P_{app} A-B \geq 2 \times 10^{-6}$  cm/s.
- (8) Salphati, L.; Lee, L. B.; Pang, J.; Plise, E. G.; Zhang, X. Role of P-glycoprotein and breast cancer resistance protein-1 in the brain penetration and brain pharmacodynamics activity of the novel phosphatidylinositol 3-kinase inhibitor GDC-0941. *Drug Metab. Dispos.* **2010**, *38*, 1422–1426.
- (9) Wager, T. T.; Chandrasekaran, R. Y.; Hou, X.; Troutman, M. D.; Verhoest, P. R.; Villalobos, A.; Will, Y. Defining Desirable Central Nervous System Drug Space through the Alignment of Molecular Properties, in Vitro ADME, and Safety Attributes. *ACS Chem. Neurosci.* **2010**, *1*, 420–434.
- (10) Wager, T. T.; Hou, X.; Verhoest, P. R.; Villalobos, A. Moving beyond Rules: The Development of a Central Nervous System Multiparameter Optimization (CNS MPO) Approach To Enable Alignment of Druglike Properties. *ACS Chem. Neurosci.* **2010**, *1*, 435–449.
- (11) Other in silico methods have been reported for the prediction of P-gp efflux. For examples, see (a) Hitchcock, S. A. Structural Modifications that Alter the P-Glycoprotein Efflux Properties of Compounds. *J. Med. Chem.* **2012**, *55*, 4877–4895. (b) Chen, L.; Li, Y.; Zhang, L.; Hou, T. Computational Models for Predicting Substrates or Inhibitors of P-glycoprotein. *Drug Discovery Today* **2012**, *17*, 343–351 and references therein.
- (12) For example, see (a) Hitchcock, S. A.; Pennington, L. D. Structure–Brain Exposure Relationships. *J. Med. Chem.* **2006**, *49*, 7559–7583. (b) Ghose, A. K.; Herbertz, T.; Hudkins, R. L.; Dorsey, B. D.; Mallamo, J. P. Knowledge-Based, Central Nervous System (CNS) Lead Selection and Lead Optimization for CNS Drug Discovery. *ACS Chem. Neurosci.* **2012**, *3*, 50–68.
- (13) Aliagas, I.; Gobbi, S. A.; Heffron, T.; Lee, M.-L.; Ortwine, D. F.; Zak, M.; Khojasteh, S. C. An in Silico Model for the Prediction of Compound Stability in Liver Microsomes. An Integrated Approach to Model Assessment and Deployment to Discovery Scientist. Unpublished results.
- (14) The CNS MPO score has also been reported to correlate with in vitro metabolic stability (ref 10). For this series of molecules, we found that our internal stability model, which had used historical program molecules as part of its training set provided a stronger correlation than CNS MPO score.
- (15) Hepatic clearance was predicted from liver microsome incubations using the in vitro  $t_{1/2}$  method: Obach, R. S.; Baxter, J. G.; Liston, T. E.; Silber, B. M.; Jones, B. C.; MacIntyre, F.; Rance, D. J.; Wastall, P. The prediction of human pharmacokinetic parameters from preclinical and in vitro metabolism data. *J. Pharmacol. Exp. Ther.* **1997**, *283*, 46–58.
- (16) Pang, J.; Baumgardner, M.; Ding, X.; Edgar, K. A.; Plise, E. G.; Wallin, J. J.; Wong, S.; Zhang, X.; Salphati, L. Preclinical Evaluation of a Novel PI3K/mTOR Inhibitor and Prediction of its Human Pharmacokinetics. *Drug Metab. Rev.* **2009**, *41*, 164 (Abstract 332).
- (17) Plots showing the change in body weight change as well as TGI for individual doses are included as Supporting Information.
- (18) The synthetic details of the remaining compounds in Table 4 are found in the Experimental Section as well as: (a) Bayliss, T.; Chuckowree, I.; Folkes, A.; Oxenford, S.; Wan, N. C.; Castanedo, G.; Goldsmith, R.; Gunzner, J.; Heffron, T.; Mathieu, S.; Olivero, A.; Staben, S.; Sutherlin, D.; Zhu, B.-Y. Phosphoinositide 3-Kinase Inhibitor Compounds and Methods of Use. WO2008/070740 A1, 2008 (b) Castanedo, G.; Dotson, J.; Goldsmith, R.; Gunzner, J.; Heffron, T.; Mathieu, S.; Olivero, A.; Staben, S.; Sutherlin, D.; Tsui, V.; Wang, S.; Zhu, B.-Y.; Bayliss, T.; Chuckowree, I.; Folkes, A.; Wan, N. C. Phosphoinositide 3-Kinase Inhibitor Compounds and Methods of Use. WO2008/073785 A2, 2008.
- (19) Tor, Y.; Del Valle, S.; Jaramillo, D.; Srivatsan, S. G.; Rios, A.; Weizman, H. Designing New Isomorphous Fluorescent Nucleobase Analogues: the Thieno[3,2-*d*]pyrimidine Core. *Tetrahedron* **2007**, *63*, 3608–3614.
- (20) Salphati, L.; Heffron, T. P.; Alicke, B.; Cheong, J.; Kharbanda, S.; Lee, L. B.; Nishimura, M.; Pang, J.; Plise, E. G.; Reslan, H. B.; Zhang, X.; Gould, S. E.; Olivero, A. G.; Phillips, H. S. Targeting the PI3K Pathway in the Brain-Efficacy of a PI3K Inhibitor Optimized to Cross the Blood–Brain Barrier. Unpublished results.
- (21) Heffron, T. P.; Berry, M.; Castanedo, G.; Chang, C.; Chuckowree, I.; Dotson, J.; Folkes, A.; Gunzner, J.; Lesnick, J. D.; Lewis, C.; Mathieu, S.; Nonomiya, J.; Olivero, A.; Pang, J.; Peterson, D.; Salphati, L.; Sampath, D.; Sideris, S.; Sutherlin, D. P.; Tsui, V.; Wan, N. C.; Wang, S.; Wong, S.; Zhu, B.-Y. Identification of GNE-477, a Potent and Efficacious Dual PI3K/mTOR Inhibitor. *Bioorg. Med. Chem. Lett.* **2010**, *20*, 2408–2411.
- (22) Pennings, M. L. M.; Reinhoudt, D. N. Chemistry of Four-Membered Cyclic Nitrones. 5. Synthesis and oxidation of 1-hydroxyazetidines. *J. Org. Chem.* **1983**, *48*, 4043–4048.
- (23) Kalvass, J. C.; Maurer, T. S.; Pollack, G. M. Use of plasma and brain unbound fractions to assess the extent of brain distribution of 34 drugs: comparison of unbound concentration ratios to in vivo p-glycoprotein efflux ratios. *Drug Metab. Dispos.* **2007**, *35*, 660–666.